Volume 10 | Number 15 | 7 August 2023

10 YEARS ANNIVERSARY

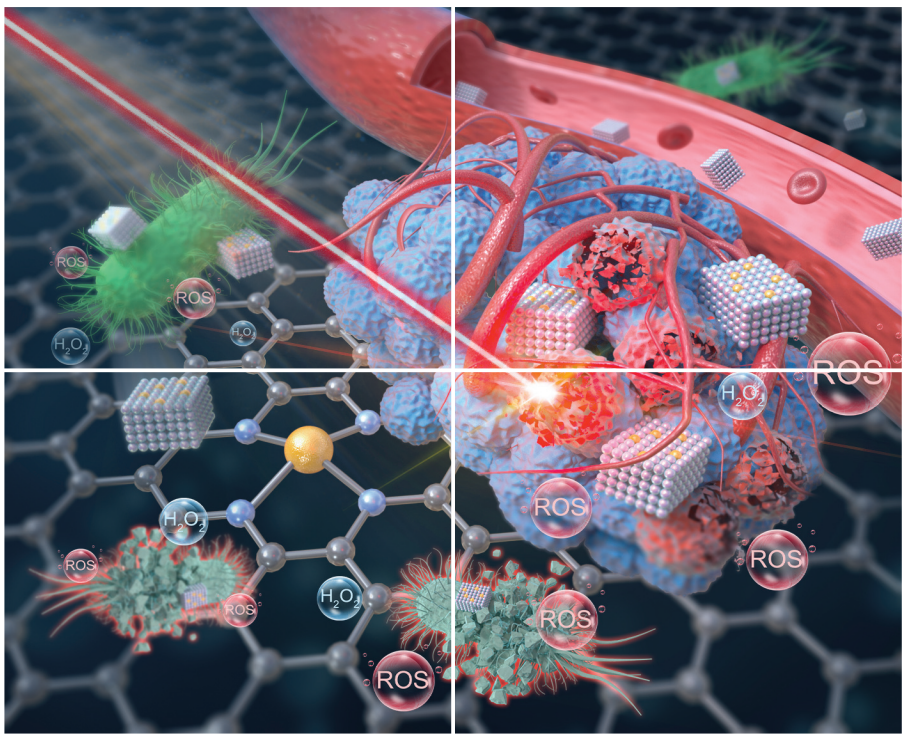


# INORGANIC CHEMISTRY

## FRONTIERS

CCS 中国化学会 CHINESE CHEMICAL SOCIETY
PEKING UNIVERSITY 1898
ROYAL SOCIETY OF CHEMISTRY
rsc.li/frontiers-inorganic

INORGANIC CHEMISTRY
FRONTIERS

CHEMISTRY FRONTIERS



**Cite this:** *Inorg. Chem. Front.*, 2023, **10**, 4289

# Single-atom nanozymes as promising catalysts for biosensing and biomedical applications

XueQian Xiao,†[a] Xiao Hu,†[a] Qiming Liu,[b] Yuling Zhang,[a] Guo-Jun Zhang *[a] and Shaowei Chen *[b]

Received 8th March 2023,
Accepted 19th April 2023

DOI: 10.1039/d3qi00430a

rsc.li/frontiers-inorganic

Nanozymes with intrinsic enzyme-like properties and excellent stability are promising alternatives to natural enzymes. Yet, their low density of active sites and unclear crystal structure have been the major obstacles that impede their progress. Single-atom nanozymes (SAzymes) have emerged as a unique system to mitigate these issues, due to maximal atomic utilization, well-defined electronic and geometric structures, and outstanding catalytic activity distinct from their nanosized counterparts. Furthermore, the homogeneously dispersed active sites and well-defined coordination structures provide rare pathways to shed light on the catalytic mechanisms. In this review, we summarize the latest progress in the rational design and engineering of SAzymes and their applications in biomedicine and biosensing. We then conclude the review with highlights of the remaining challenges and perspectives of this emerging technology.

## 1. Introduction

Enzymes are biocatalysts produced by living cells that possess a high catalytic activity promoting specific biological reactions in the body and maintain cell life activities. Most enzymes are proteins (a small number are RNA); their catalytic activities can be greatly impacted by the chemical environment, as enzymes are prone to degradation, and the high cost of preparation makes large-scale production difficult. To mitigate these issues, artificial enzymes have been attracting extensive attention as stable and low-cost alternatives.[1,2] In 2007, Yan *et al.* found that $Fe_3O_4$ nanoparticles exhibited peroxidase (POD)-like activity and the optimal catalytic conditions were approximate to those of natural horseradish peroxidase (HRP), which was a significant breakthrough in the field of nanomaterials biocatalysis.[3] Since then, the term "nanozyme" has attracted widespread attention,[4–6] due largely to high stability, low cost, tuneable catalytic activity, and ease of large-scale production.[7,8] There are three major types of nanozymes based on their substrates: carbon-based nanozymes, metal-based

[a]*School of Laboratory Medicine, Hubei University of Chinese Medicine, 16 Huangjia Lake West Road, Wuhan, Hubei 430065, China. E-mail: zhanggj@hbtcm.edu.cn*
[b]*Department of Chemistry and Biochemistry, University of California, 1156 High Street, Santa Cruz, California 95064, USA. E-mail: shaowei@ucsc.edu*
† These authors contributed equally to the work.

**Xueqian Xiao**

*XueQian Xiao received her B.S. degree in Medical Laboratory Technology from Hubei University of Chinese Medicine (HUCM), Wuhan, China, in 2022. She is currently pursuing an M.S. degree under the supervision of Prof. Guo-Jun Zhang at HUCM.*

**Xiao Hu**

*Hu Xiao obtained her Bachelor's and Master's degrees from HUCM in 2010 and 2013, respectively. Currently, she is pursuing her Doctor's degree under the supervision of Prof. Zhang Guo-Jun at HUCM. Her research focuses on nano-biosensor development and biomarker detection.*

nanozymes, and metal oxide-based nanozymes,[9] featuring catalytic activities resembling those of natural enzymes like POD, oxidase (OXD), catalase (CAT), superoxide dismutase (SOD), glucose oxidase (GOx) and hydrolase.[10–12] Thus far, nanozymes have been widely adopted in diverse fields, such as disease diagnosis and treatment, biosensing, food safety, environmental monitoring, and chemical production, among others.[13–15]

Whereas nanozymes may possess properties that are superior to those of natural enzymes, the catalytic activity and substrate affinity remain mostly subpar compared with those of natural enzymes. This is mainly attributed to the low density of active sites in nanozymes, and their unclear crystal structure and complex elemental composition make it difficult to unravel the catalytic mechanisms.[16,17] To overcome these barriers, single-atom nanozymes (SAzymes) have emerged as a unique platform, where the catalytic activity can be enhanced by the maximal utilization of metal atoms and the well-defined atomic configuration offers unprecedented insights into the mechanistic origin.[18]

In SAzymes, isolated metal atoms are anchored onto a select structural scaffold and the resultant coordination moiety serves as the active centers (Fig. 1).[19,20] SAzymes combine the advantages of homogeneous catalysts and heterogeneous catalysts, and may break the limitations in material design for unprecedented catalytic activity.[21,22] In most studies, SAzymes exhibit POD- and OXD-like activity,[23–25] and can break down $H_2O_2$ to reactive oxygen molecules (ROS) that are potent agents in the inhibition of the growth of harmful cells such as bacteria and viruses.[26–28] Meanwhile, by deliberate manipulation of the coordination structure between the metal atoms and the supports, the SAzyme active centers can be carefully tailored, leading to multienzyme catalytic activity for enzyme cascade reactions,[29,30] and a catalytic performance competitive with that of the natural enzyme.[31] Meanwhile, the well-defined active sites and electronic properties make it possible to reveal the structure–activity correlation.[32–34] In addition, the development of effective synthetic strategies, such as wet impregnation and high-temperature annealing, have made possible the large-scale preparation of SAzymes with a high metal coverage and stable metal coordination structure, as compared to conventional synthesis methods.[35] The structural insights can also be exploited for the construction of relevant models for theoretical calculations where further insights into the mechanistic origin can be obtained.[36]

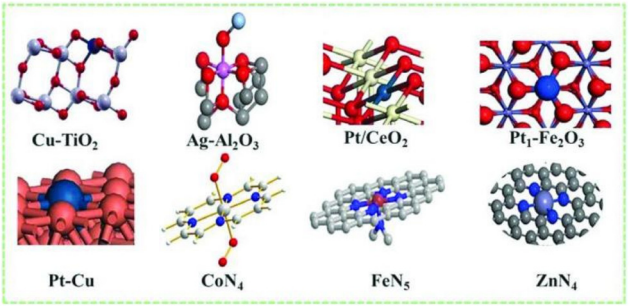


**Fig. 1** Representative SAzymes with metal centers homogeneously dispersed within a range of supporting scaffolds, such as carbon, metal oxides, and metals. Reproduced with permission from ref. 20, copyright 2020, Royal Society of Chemistry.

In this review, we will summarize the latest progress in the design and synthesis of SAzymes and their applications in biomedicines and biosensing, highlight the remaining challenges and put forward opportunities in future research (Scheme 1).

## 2. Synthetic strategies

Experimentally, a range of structural parameters, in particular, the coordination configuration of the metal centers and the geometric structure of the supporting substrates, have been found to impact the catalytic performance of SAzymes. This may consist of the manipulation of the crystal plane, surface coating, elemental composition, heteroatom doping, and selection of cofactor mimics, among others.[37] Thus far, a great

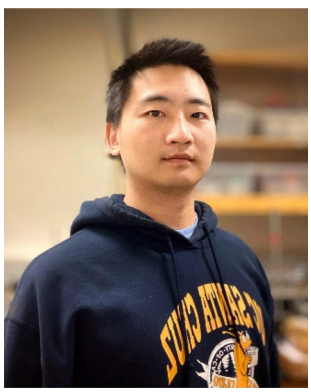

**Qiming Liu**

*Qiming Liu received his B.E. degree in Materials Chemistry in 2018 from Central South University, Hunan, China. He then joined Professor Shaowei Chen's group at UCSC to pursue a Ph.D. degree in Chemistry. His research interests concentrate on the design and engineering of nanocomposite catalysts for electrochemical energy conversion, development of ultrafast synthesis, and ligand functionalization of nanoparticles.*

**Yuling Zhang**

*Yuling Zhang obtained his Bachelor's degree in 2004 and Ph.D. degree in 2013 from Wuhan University. Currently, he is an associate research fellow at HUCM. His research interest is focused on early diagnosis of diseases* via *biosensing of disease-related biomarkers.*

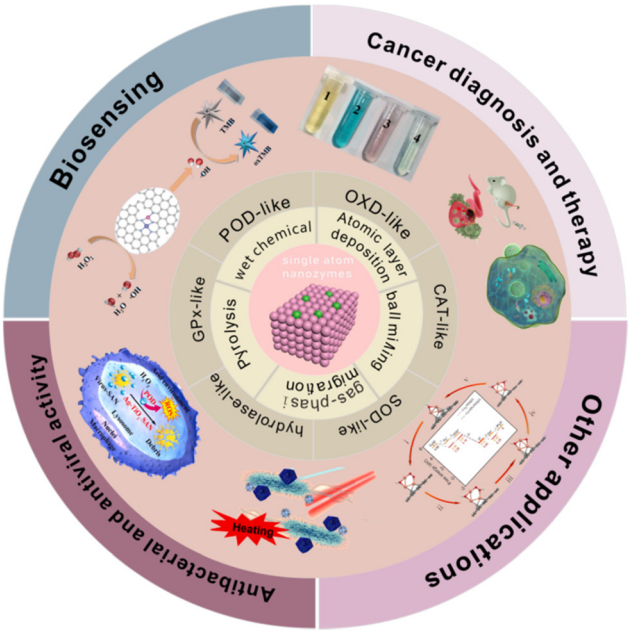


**Scheme 1** Schematic illustration of SAzymes for a broad scope of biologically critical applications.

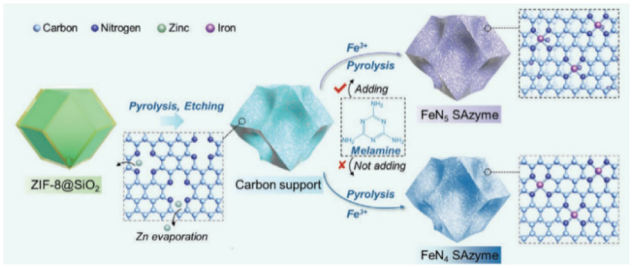


**Fig. 2** Schematic illustration of the synthesis of $FeN_5$ SAzyme from a ZIF-8 precursor. Reproduced with permission from ref. 55, copyright 2022, Wiley.

many SAzymes have been successfully prepared *via* both bottom-up and top-down synthetic procedures. The former mainly involves atomic layer deposition (ALD),[38,39] ball milling,[40,41] wet chemistry,[42,43] mass-selected soft landing,[44,45] and photochemical reduction,[46,47] while the latter entails high-temperature pyrolysis[48,49] and gas-phase migration.[50,51] Below is a summary of these synthetic methods.

Pyrolysis is a widely used method for the synthesis of SAzymes.[52] Experimentally, a metal salt precursor is incorporated into a select organic matrix (typically containing nitrogen). The mixture is then pyrolyzed at elevated temperatures under an inert atmosphere, where the nitrogen atoms are doped into the resulting carbon scaffold and the metal atoms form an M–N–C coordination structure with the carbon and nitrogen atoms (*e.g.*, M = Fe, Cu, Co, Zn, Mn, *etc.*).[53] Among these, metal–organic frameworks (MOFs) are the commonly used support materials due to their structural diversity and functional tunability.[54] Under high temperature and inert atmosphere, the organic ligands are carbonized and the metal nodes within the MOFs are converted into metal sites uniformly dispersed within the carbon support. For example, zeolitic imidazole framework-8 (ZIF-8) has been used as a precursor for the preparation of Fe SAzymes consisting of $FeN_4$ and $FeN_5$ active sites through a melamine-mediated two-step pyrolysis strategy, where the coating of a $SiO_2$ shell inhibits nanoparticle aggregation during high-temperature pyrolysis (Fig. 2).[55]

However, pyrolysis at high temperatures usually produces metal (oxide)-containing nanoparticles, resulting in a heterogeneous structure. Note that whereas the nanoparticles may be removed by, for instance, acid etching, the removal is generally incomplete.[56] In addition, during pyrolytic treatment of MOFs, the framework structure may collapse,

**Guo-Jun Zhang**

*Guo-Jun Zhang received his Ph.D. degree in Medicine in 1999 from Tongji Medical School of Huazhong University of Science and Technology, China. He was a Postdoctoral Fellow at Wuhan University (1999–2000), a DAAD Postdoctoral Fellow at the Institute for Physical High Technology, Jena, Germany (2001–2002), a JSPS Postdoctoral Fellow (2002–2004), Visiting Lecturer (2004) and Visiting Associate Professor (2005) at Waseda University, Japan, and a Member of the Technical Staff at the Institute of Microelectronics, Singapore (2006 to 2011). He is currently a Professor at HUCM, working on the fabrication of nano-biosensors and their medical applications.*

**Shaowei Chen**

*Shaowei Chen finished his undergraduate study in 1991 with a B.S. degree in Chemistry from the University of Science and Technology of China (USTC), and then went to Cornell University, receiving his M.S. and Ph.D. degrees in 1993 and 1996, respectively. Following a postdoctoral appointment at the University of North Carolina at Chapel Hill, he started his independent career at Southern Illinois University in 1998. In the summer of 2004, he moved to UCSC, and is currently a Professor of Chemistry and the Faculty Director of the UCSC COSMOS program.*

leading to rearrangement of the carbon skeleton, which complicates the structure and compromises the accessibility of the M–N–C moiety.

Wet-chemistry strategies have also been employed extensively for SAzyme synthesis.[57,58] In such procedures, metal-containing precursors are immobilized onto a suitable support *via* impregnation, co-precipitation, ion exchange or electrostatic absorption, followed by drying and calcination to remove the undesired ligands. In the wet-chemistry procedures, it is important to strengthen the interactions between the metal atoms and the support, and concurrently prevent the aggregation of the metal atoms. This can be achieved with a substrate containing carbon, oxygen and nitrogen, due to strong binding of the metal atoms. This can be further enhanced with structural defects on the support's surface. Indeed, defect engineering can be exploited for the ingenious design of the coordination structures and hence manipulation of the catalytic activity. Notably, the obtained SAzymes can be readily dispersed in aqueous media; yet, a large size may impede the *in vivo* activity.[35,59]

ALD is another effective strategy to prepare SAzymes, and is based on a series of continuous self-limiting reactions occurring between the surface of an active precursor substance and an active substrate material.[60] The self-limiting characteristics promote the spontaneous formation of a regular geometric structure of SAzymes, a unique feature for studying the correlation between the materials structure and catalytic activity.[61]

Other methods, such as atom trapping[62] and gas-phase migration,[63] are also emerging. These allow the development of a diverse range of experimental methods for SAzyme preparation.

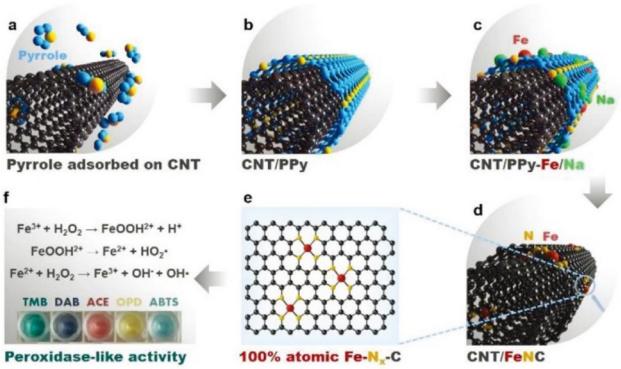


**Fig. 3** Schematic illustration of the synthesis and catalytic mechanism of Fe SAzymes using carbon nanotubes as a support substrate. (a) Adsorption of pyrrole molecules on CNT through π–π interactions. (b) Addition of ammonium peroxydisulfate induces pyrrole polymerization to obtain polypyrrole-coated CNT (CNT/PPy). (c) Adsorption of metal cations on CNT/PPy from the solution of $Fe(NO_3)_3$ and NaCl. (d) CNT/FeNC SAzyme obtained by pyrolysis of CNT/PPy with adsorbed metal ions in $N_2$ and then $NH_3$. (e) Fe–$N_x$–C moieties in CNT/FeNC SAzyme. (f) POD activity of CNT/FeNC SAzyme in catalyzing the Fenton reaction to generate hydroxyl radicals (·OH). This can be exploited for the oxidative degradation of 3,3′,5,5′-tetramethylbenzidine (TMB, blue), di-azo-aminobenzene (DAB, gray), 3-amino-9-ethylcarbazole (AEC, red), *o*-phenylene diamine (OPD, yellow), and 2,2′-azino-bis(3-ethylbenzothiazoline-6-sulfonic acid) diammonium salt (ABTS, green). Reproduced with permission from ref. 70, copyright 2019, Wiley.

## 3. SAzyme supports

Due to a high surface free energy, metal atoms tend to aggregate into nanoclusters or nanoparticles. It is therefore vital to select an appropriate supporting substrate to stabilize the individual metal atoms and prevent their aggregation. Within this context, two structural scaffolds have been used in the preparation of SAzymes, one carbon-based and the other noncarbon-based.[64]

### 3.1 Carbon-based supports

Carbon-based supports mostly consist of graphene, graphene oxide, carbon nanotubes (CNTs), MOFs, and graphitic carbon nitride (g-$C_3N_4$). These supports are usually doped with N atoms, and can thus be used to form the $MN_x$ coordination moiety with the metal atoms (M = Fe, Cr, Zn, Mn, Cu, *etc.*).[65–68] The exposed area of the active sites and the electron-transfer dynamics can be enhanced by the formidable metal–support covalent coordination.[69] For instance, Cheng *et al.*[70] designed a CNT-supported SAzyme (CNT/FeNC) consisting of $FeN_x$ moieties, by using NaCl crystals as the removable templates (Fig. 3). The CNT/FeNC SAzyme catalyzed the decomposition of $H_2O_2$ to hydroxyl radicals (·OH) *via* the Fenton reaction. This POD-like activity was superior to those of $Fe_3O_4$ nanoparticles and other Fe-based nanozymes reported earlier. In another study, inspired by the actual shape of the heme cofactor of natural HRP, Lee *et al.*[71] designed and synthesized $FeN_4$ single-site-embedded graphene (Fe–N-rGO), and observed a high enzymatic activity and selectivity, which was confirmed by density functional theory (DFT) calculations.

g-$C_3N_4$ is another effective supporting substrate for SAzymes, which exhibit preeminent POD-like activity in the generation of ·OH from $H_2O_2$ decomposition.[72,73] However, pristine g-$C_3N_4$ usually show a poor catalytic performance owing to defects in the shape and internal structure.[74,75] Thus, a sharp-tip nanoneedle structure has been designed in order to alleviate the impediment of electron transfer by bulk g-$C_3N_4$ structure.[76] For instance, Fan *et al.*[77] fabricated a 3D branched g-$C_3N_4$ artificial enzyme through the ionothermal assay. The unique sharp-edge morphology formed by the modified synthetic process improved the crystallinity of g-$C_3N_4$, reduced charge-transfer resistance and accelerated $H_2O_2$ activation. The performance of g-$C_3N_4$ can also be enhanced by metal or nonmetal doping. Jiang *et al.*[78] prepared g-$C_3N_4$ composed of sulfur-doped and sulfur-free active sites *via* liquid sulfur-mediation, where the doping of sulfur atoms led to a significant improvement of the catalytic performance. Likewise, the deposition of noble metal atoms (such as Pt, Pd, and Au) was found to induce localized surface plasmon resonance (SPR) which played a vital role in enhancing the catalytic activity.[79] In fact, defect engineering,[80] modification tactics,[81] and het-

erojunction construction[82] have been employed to improve the catalytic performance of g-$C_3N_4$.

MOFs, another important class of carbon-based supports, are coordination polymers that possess a porous and periodic network structure formed by the self-assembly of transition metal ions and organic ligands, and hence a large specific surface area and tuneable pore size. This enables intimate contact between the substrates and metal atoms and endows MOFs with artificially designed active sites and adjustable catalytic activity.[83,84] Indeed, MOF-based bioinspired nanomaterials with unique chemical activities, such as photodynamic, sonodynamic, and enzyme-like activities, have found diverse biomedical applications, including tumor therapy, antibacterial therapy and antioxidant therapy (Fig. 4). For instance, four pyrrolic nitrogen sites can form a plane-square structure, which is similar to a porphyrin motif. The center of the four sites acts as a solid trap to bind metal atoms and the surrounding N containing electron lone pairs as donors to coordinate with the target metal atoms.[85,86] Compared with metal-free porphyrins, metalloporphyrin-based organic linkers containing $MN_x$ sites are formed when the two pyrrole protons (N–H) in the rigid macrocycles of porphyrin are replaced by metal ions, which display enhanced catalytic activity due to the optimized electronic structure and accelerated electron transfer.[87] Therefore, MOFs with different structures and functions can be constructed through self-assembly between metal nodes and porphyrin-based organic linkages, such as tetrakis (4-carboxyphenyl)porphyrin ($H_2$TCPP), 5,10,15,20-tetrakis(4-aminophenyl)porphyrin (TAPP), 5,10,15,20-tetrakis(4-pyridyl) porphyrin ($H_2$TPyP), (dicarboxyphenyl)porphyrin (BDCPP), and so on.[88] For example, manganese porphyrin-based MOFs (Mn-MOFs) have been found to exhibit unique SOD- and CAT-like activity, which can remove superoxide anion free radicals, and have been used in tumor immunotherapy and nanovaccine fields.[89]

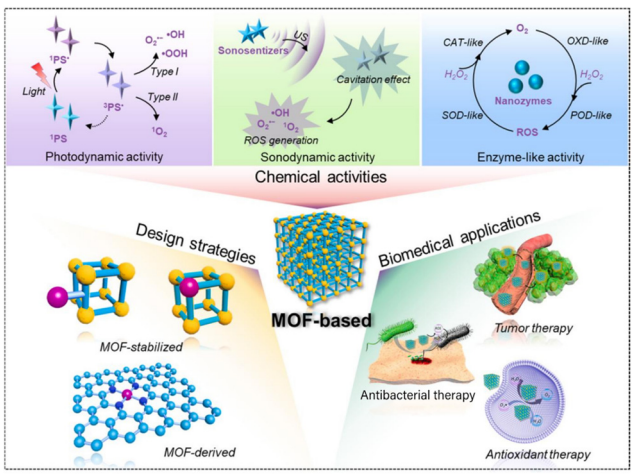


Fig. 4 Design strategies and biomedical applications of MOF-based bioinspired nanomaterials with chemical activities. Reproduced with permission from ref. 84, copyright 2023, Elsevier.

Extensive research efforts have also been devoted to covalent organic framework (COFs).[90] The 2D structure of COFs furnishes a high-ordered arrangement and conjugated skeleton, along with a number of hollow sites for stable anchoring of transition-metal centers.[91] For instance, Dong *et al.*[92] prepared a 2D COF where the periodic organic building blocks were used to stabilize Pt single atoms while the heteroatom-rich (C, N, and O) pore walls afforded unique coordination environments to increase metal atom loading, leading to an increase of the active sites and catalytic activity. In another study,[93] Liu's group prepared a bipyridine-rich COF conjugated with Co single atoms *via* out-of-plane coordination. Note that in recent years, the COF-derived products have mostly been used for photocatalytic applications,[94,95] with few as biological enzymes.[96] Further research is strongly desired.

### 3.2 Noncarbon-based supports

Noncarbon-based supports also attract great attention. Among these, transition metal oxide nanomaterials have become one of the most promising scaffolds.[97] Structural defects on the surface of metal oxides can act as binding sites for anchoring single metal atoms. Meanwhile, the distinctive crystal phases and rich electron configurations afford opportunities to form different coordination structures between the metal atoms and scaffolds. Indeed, a great quantity of transition metal oxide-based SAzymes have been prepared. Among these, $TiO_2$ has been used extensively as a support material, due to strong interactions with the metal atoms. Notably, Qiao's group prepared a Pt-$TiO_2$ SAC and noticed that the metal–support interaction stemmed from the coordination environment rather than physical adsorption or sedimentation.[98] In fact, the metal oxide supports not only immobilize the dispersed metal atoms but also stabilize the geometric structure and modify the electronic structure, which can boost the catalytic performance.[99] Mechanistically, the lattice confinement in the internal structure of the supports acts as substitutable sites for the target metal atoms. In contrast to the defect-stabilized structure, lattice-confined sites can be replaced more easily.[100] Jiang's group synthesized a Pd/$MnO_2$ SAC with lattice-restricted structures, owing to the spatial constraint of Pt atoms by $MnO_2$, which spontaneously extracted surrounding lattice oxygen at room temperature with an ultralow energy barrier.[101] The unique coordination environment formed by the metal atoms and metal oxide supports can significantly boost the catalytic activity towards a range of reactions, such as the carbon monoxide oxidation reaction and the decomposition reaction of hydrogen peroxide.

Transition metal sulfides have also served as effective supports. For instance, cobalt can be atomically dispersed onto a $MoS_2$ scaffold, and the resultant Co-$MoS_2$ SAzyme exhibits apparent POD-like activity.[102] In summary, appropriate supports play a critical role in tuning the active sites, improving the catalytic performance and biological applications of SAzymes, which will be highlighted below.

# 4. Enzymatic activity of SAzymes

A range of SAzymes have been prepared and used in diverse applications, in particular, biosensing and diagnostics. The metal center is an integral part of the SAzymes, which forms an M–N–C coordination moiety with surrounding N atoms through metal–N δ bonds that mimic the enzyme active centers.[103] Different valence states and electronic structures of the metal atoms give rise to different coordination configurations, and therefore the catalytic activity is closely related to the electron density, size[104] and number[105] of the metal centers. In fact, experimentally, the catalytic activity, selectivity and biological performance can be effectively regulated by manipulation of the metal species, coordination environment, heteroatomic doping and surface modification.[36] Below, we will summarize the development of leading SAzymes within the context of the metal centers (Table 1).

## 4.1 Fe SAzymes

Fe-centered SAzymes, one of the most promising mimetic enzymes, have been extensively studied in recent decades, where the Fe–N–C coordination moiety serves as the active center due to geometric and electronic effects.[106] Among the numerous strategies for synthesis, controlled pyrolysis of zeolitic-imidazolate frameworks (*e.g.*, ZIF-8) has been the leading method in recent years for the preparation of Fe SAzymes. For instance, Lin's group[107] prepared a $FeN_4$ SAzyme by pyrolysis of ZIF-8 and observed an unprecedented POD-like activity. Motivated by the structure of hemoglobin, Liu *et al.*[108] designed a precursor including hemin and ZIF-8 (Hemin@ZIF-8). During pyrolysis hemin served as the doping agent and effectively suppressed the aggregation of Fe atoms. Meanwhile, the larger hemin would burst the cage of ZIF-8 and break the confinement effect, creating a microporous multilayer structure and a high surface area. Experimentally, the group synthesized a series of Fe,N co-doped porous carbon, and observed that the POD-like activity in the TMB oxidation reaction varied with the initial feed of hemin, among which an optimal loading was identified.[109] Another noteworthy example is spherical mesoporous Fe–N–C SAzyme, which featured a large pore size (4.0 nm), high specific surface area (413.9 $m^2\ g^{-1}$), uniform diameter (100 nm) and highly dispersed iron atoms.[110] These characteristics facilitated mass transport and accessibility of the active sites, and hence boosted the POD-like activity.

In a recent study,[111] we developed an Fe SAzyme platform for glucose sensing with a dual-signal readout mode based on fluorescence and electrochemistry. Experimentally, 3D porous N-doped carbon aerogels were used as the support matrix in which Fe single atoms were embedded to achieve uniform dispersion and maximize atomic utilization. Specifically, with $SiO_2$ nanoparticles as the structural templates, a gelatin-zinc hydrogel containing iron(II) phenanthroline ($Fe(PM)_3^{2+}$) was exploited as the precursor and subjected to repeated freeze-

**Table 1** Summary of leading SAzymes with different metal centers

| Coordination structure | Synthetic method | Characterization | Enzyme-like activity | Biomedical applications | Ref. |
|---|---|---|---|---|---|
| $Fe–N_4$ | Pyrolysis | TEM, XRD | POD | Biosensing | 107 |
| $Fe_{55}$–N–C | Chemical coprecipitation and pyrolysis | SEM, TEM, HRTEM HAADF-STEM, XPS, XRD | POD | Biosensing | 108 |
| Fe–N–C | Wet-chemistry and high-temperature calcination | SEM, TEM, HRTEM, STEM, XPS, XRD | POD | Antibacterial therapy | 110 |
| $Fe–N_4$ | Pyrolysis and etching | TEM, STEM, XRD, XPS | GOx and HRP | Biosensing | 111 |
| $Fe–N_5$ | Hydrothermal synthesis | TEM, HAADF-STEM | OXD | Biosensing and antibacterial therapy | 112 |
| Co–N–C | Wet-chemistry | SEM, TEM, XRD | POD | Biosensing | 114 |
| Co–N–C | Hydrothermal and pyrolysis | TEM, HRTEM, STEM, XPS, XRD | OXD | Biosensing | 115 |
| Co–N–C | Coordination–pyrolysis–corrosion | TEM, HAADF-STEM, XANES, EXAFS | CAT | Cancer therapy | 116 |
| Zn–N–C | Pyrolysis | TEM, HAADF-STEM, XPS, XRD, EXAFS | POD | Biosensing and antibacterial therapy | 118 |
| Pt–N–C | Ionothermal method | SEM, TEM, HAADF-STEM, XPS | POD | $H_2O_2$ detection and antibacterial therapy | 128 |
| Cu–N–C | Wet-chemistry | TEM, XRD, XPS | POD, OXD | Antibacterial therapy | 130 |
| $Cu–N_4$ | Electrochemical deposition | TEM, HAADF-STEM, EXAFS, XANES, XRD, XPS | Ascorbate peroxidase-like (APX-like) | Anti-oxidative damage | 27 |
| $Ru–C_6$ | *In situ* one-pot multicomponent self-assembly | SEM, TEM, HAADF-STEM, XRD, XPS, NEXAFS | POD | Cancer therapy | 164 |
| Mn–N–C | Etching–adsorption–pyrolysis | TEM, HAADF-STEM, EXAFS, XANES, XAFS, XRD, XPS | CAT, OXD, POD | Cancer therapy | 171 |
| Pd–N–C | "Top-down" strategy | TEM, HRTEM, HAADF-STEM, EXAFS, XANES, XRD, XPS | POD, GSHOx-mimic | Cancer therapy | 165 |

TEM, transmission electron microscopy; HRTEM, high-resolution transmission electron microscopy; HAADF-STEM, high-angle annular dark field-scanning transmission electron microscopy; SEM, scanning electron microscopy; XRD, X-ray diffraction; XPS, X-ray photoelectron spectroscopy; EXAFS, extended X-ray absorption fine structure; XANES, X-ray absorption near-edge spectroscopy.

drying at −20 °C. The resulting biomass hydrogel was then transformed into N-doped carbon aerogel anchored with Fe single atoms (NCAG/Fe) by pyrolysis and acid etching, which possessed a large surface area and rich mass transport channels and exhibited outstanding POD-like properties due to the formation of $FeN_4$ moieties. In fact, nonfluorescent OPD could be oxidized to fluorescent 2,3-diaminophenazine (DAP) by $H_2O_2$ generated by NCAG/Fe-catalyzed oxidation of glucose, and the fluorescence signal intensity varied with the glucose concentration; concurrently the oxidation of glucose also generated a significant electrochemical signal. Such a dual-signal detection platform could be exploited for the accurate and reliable detection of glucose even in clinical serum samples and artificial body fluids, as compared with commercial sensors.

Notably, Fe SAzymes may consist of not only $FeN_4$ but also $FeN_5$ coordination moieties, and the latter show a better catalytic activity, owing to the optimized coordination structure. For instance, inspired by the axial ligand-coordinated heme of cytochrome $P_{450}$, Huang *et al.*[112] rationally introduced a fifth nitrogen atom into the structure of $FeN_4$ to form axial coordination with the central iron atom. In the new assay, the organic nitrogen linkers were converted to pyridinic nitrogen at high temperature, which coordinated with the $FeN_4$ sites that were separated under the constraint of the carbon nanoframes (Fig. 5a). The axial-coordination N atom of $FeN_5$ effectively activated $O_2$ and facilitated the cleavage of the O–O bond, behaving like natural oxide enzymes. At the same time, the authors systematically studied a series of nanozymes with a similar $MN_5$ structure (M = Co, Mn, Ni, and Cu), from which $FeN_5$ SA/CNF was found to exhibit the highest OXD-like activity, stability and biocompatibility (Fig. 5b–d). Results from DFT calculations were highly consistent with the experimental conclusion. Taken together, these results show that the emergence of $FeN_5$ SAzymes provides a valuable reference in uncovering and understanding the enzyme-like mechanism and paves the way for ingenious formulation and appropriate applications of SAzymes.

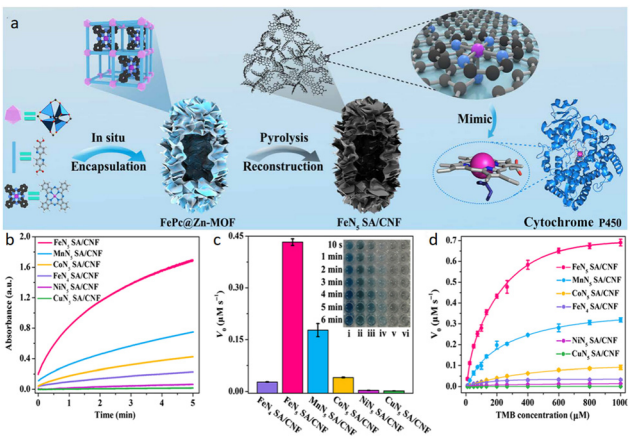


**Fig. 5** (a) Schematic formation process of carbon nanoframe-confined atomically dispersed Fe sites with axial N coordination for mimicking the active center of cytochrome $P_{450}$. (b) Comparison of the OXD-like activity of a series of nanozymes with a similar $MN_5$ structure (M = Co, Mn, Ni, and Cu), as manifested by the time-dependent absorbance of oxidized TMB (oxTMB) at 652 nm. (c) Histogram of the initial reaction rate ($V_0$) and (d) typical Michaelis–Menten curves in the presence of (i) $FeN_5$ SA/CNF, (ii) $MnN_5$ SA/CNF, (iii) $CoN_5$ SA/CNF, (iv) $FeN_4$ SA/CNF, (v) $NiN_5$ SA/CNF, and (vi) $CuN_5$ SA/CNF in air-saturated sodium acetate–acetic acid buffer. The inset to (c) is the photographs of the TMB solution in the presence of the various catalysts for up to 6 min. Reproduced with permission from ref. 112, copyright 2019, AAAS.

### 4.2 Co SAzymes

As with the heteromorphism of $Fe_3O_4$, the enzyme-like properties of $Co_3O_4$ nanoparticles have attracted wide attention, where the catalytic activity can be improved by changing the shape and increasing the specific surface area.[113] For instance, Wang's group[102] used the single-atom Co-$MoS_2$ nanozymes as a model, and combined experimental and theoretical studies to show that the Co centers and the $MoS_2$ supports involved different catalytic mechanisms: the former entailed an electron-transfer mechanism, while the latter was based on a Fenton-like reaction. The synergistic interactions between the Co single atoms and $MoS_2$ substrates greatly improved the POD-like activity of Co-$MoS_2$, which was successfully applied in the colorimetric and electrochemical sensing of hydrogen peroxide.

In another study,[114] Co SAzymes were pyrolytically derived from ZIF-67 and a cobalt salt template featuring unsaturated Co-porphyrin centers, and the resultant Co-PMCS SAzymes exhibited excellent POD-like and other enzyme-like activities. This was then exploited for the colorimetric detection of a series of antioxidants by taking advantage of the color change of TMB oxidation by $H_2O_2$ catalyzed by the Co-PMCS SAzyme, where the color diminished in the presence of various antioxidants. The sensor assay was demonstrated with 7 antioxidants, and exhibited a low detection limit, high accuracy, and good anti-interference capability. Sun's group exploited the inhibition of the OXD-like activity of Co–N–C SAzymes by thiols for the detection of biothiols (*e.g.*, glutathione (GSH), cysteine (Cys)),[115] as biothiols could bind to the Co centers, inhibit the adsorption of $H_2O_2$, and thus block the oxidation process. Chen's group prepared a Co-SAs@NC SAzyme *via* a coordination–pyrolysis–corrosion process and observed CAT-like activity.[116] In the tumor microenvironment, the SAzyme first acted as a CAT to decompose the endogenous $H_2O_2$ of tumor cells to $O_2$, and then functioned as an OXD to catalyze the conversion of $O_2$ into highly cytotoxic $O_2^{\bullet-}$ radicals which led to apoptosis of the tumor cells.

In a recent study,[117] following the previous procedure for the preparation of NCAG/Fe, we synthesized a Co SAzyme based on the similarly structured N-doped carbon aerogels. Again, the gelatin-zinc hydrogel was adopted as the precursor, into which were added a Co-PM complex and $SiO_2$ nanoparticles. The hydrogel was then pyrolytically converted into honeycomb carbon aerogels embedded with Co single atoms (NCA-Co) consisting of three active sites, $CoN_4$ in the basal plane, as well as $CoN_4$ and $CoN_3$ at the edge of the aerogel

nanopores (Fig. 6a). Theoretical calculations showed that the adsorption energy of glucose at the different metal sites varied in the order of basal $CoN_4$ (−1.047 eV) < nanopore-edge $CoN_3$ (−0.811 eV) < nanopore-edge $CoN_4$ (−0.634 eV), suggesting the high catalytic activity of cobalt sites at the nanopore edges. When the NCA-Co nanozyme was used for electrochemical detection of glucose, good linearity was observed between the glucose concentration and current signal, due to the POD-like activity of the NCA-Co SAzyme (Fig. 6b–g).

### 4.3 Zn SAzymes

ZIFs are a kind of MOF with a zeolite-like framework structure, which are produced by the reaction of metal ions, such as divalent Zn and Co, and imidazole or their derivative ligands in organic solvents. Among them, zinc-based ZIF-8 is the most commonly used ZIF and can be used to derive carbon nanocomposites containing atomically dispersed zinc atoms (Fig. 7a).[118] With the addition of target metal ions of a similar size to $Zn^{2+}$ (*e.g.*, $Co^{2+}$, $Ni^{2+}$, $Fe^{2+}$, *etc.*), the target metal ions can be homogeneously distributed into the metal nodes of the ZIF framework to form bimetallic ZIFs through coordination with the 2-methylimidazole linker. As the Zn species become

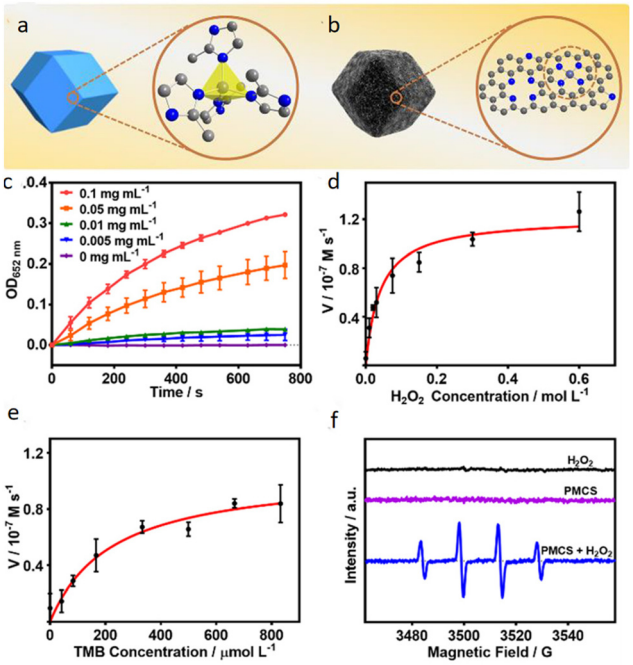


**Fig. 7** (a) Schematic illustrations of ZIF-8 with the $ZnN_4$ tetrahedral motif and (b) PMCS with the porphyrin-like structural model. (c) POD-like activity of PMCS at different concentrations in the catalytic oxidation of TMB. Steady-state kinetic assay of PMCS for (d) $H_2O_2$ and (e) TMB. (f) ESR spectra demonstrating $^{\bullet}OH$ generation by $H_2O_2$, PMCS, and PMCS + $H_2O_2$. Reproduced with permission from ref. 118, copyright 2019, Wiley.

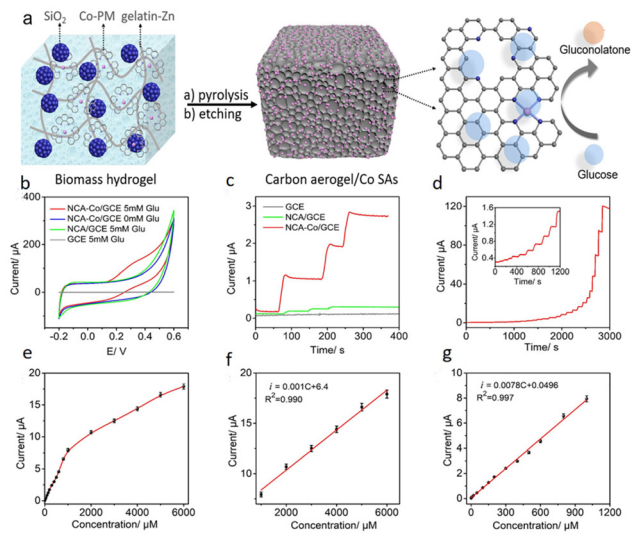


**Fig. 6** (a) Schematic of the preparation of NCA-Co aerogels derived from biomass hydrogels. (b) Cyclic voltammograms in 0.1 M NaOH at the scan rate of 50 mV $s^{-1}$ of NCA-Co/GCE (GCE, glassy carbon electrode) in the absence and presence of 5 mM glucose, NCA/GCE and bare GCE in the presence of 5 mM glucose. (c) Chronoamperometric profiles of different modified electrodes at the applied potential of +0.3 V with the successive additions of 100 μM glucose into 0.1 M NaOH. (d) Chronoamperometric curve of the NCA-Co/GCE electrode upon the successive addition of glucose at various concentrations (0.5, 1, 2, 10, 20, 50, 100, 150, 200, 300, 400, 500, 600, 800, 1000, 2000, 3000, 4000, 5000, 6000 μM) into a 0.1 M NaOH solution at the applied potential of +0.3 V. Inset is the magnified segment for the glucose concentration range of 0.5 to 100 μM. (e) Current signals at different glucose concentrations and the corresponding linear correlation between the oxidation current increment and glucose concentration in the range of (f) 0.5–1000 μM and (g) 1000–6000 μM. Reproduced with permission from ref. 117, copyright 2022, Elsevier.

evaporated at high temperatures, porous carbon is formed and embedded with the target metal ions. For ZIF-8-derived carbon (Fig. 7b), the Zn-centered porphyrin-like moiety endows the sample (denoted as PMCS) with a POD-like activity, as manifested in the catalytic oxidation of TMB in the presence of $H_2O_2$ (Fig. 7c–e). The unsaturated $ZnN_4$ coordination configuration acts as active sites and can catalyze the decomposition of $H_2O_2$ into hydroxyl radicals ($^{\bullet}OH$), as confirmed in electron spin resonance (ESR) measurements (Fig. 7f). The optimal reaction conditions are similar to those for HRP, and the high activity can be retained within a wide range of pH and temperature. Xu *et al.*[119] synthesized Mo/Zn dual-atom nanozymes supported on a macroscopic amphiphilic aerogel by pyrolysis of poly(vinyl alcohol) (PVA) and supramolecular coordination complexes.[120] The macroscopic dimension of the PVA substrate not only greatly enhanced the metal atom loading, but also stabilized the metal atoms. The Zn/Mo dual SAzyme showed a high metal content (1.5 and 7.3 wt% of Zn and Mo, respectively) without acid etching and with no structural collapse of the support, and synergistically led to a POD-like activity.

Of the Zn-based nanocomposites, the $ZnN_4$ moieties have been known to exhibit a high catalytic activity since the N atoms coordinating to the Zn center significantly lower the energy barrier and accelerate the electron-transfer kinetics. In fact, Zn SAzymes have shown potent antibacterial activity without external stimulation and toxicity to tissues and organs, in contrast to their nanoparticle forms.[121,122]

### 4.4 Pt SAzymes

Since the first report from Zhang' group that Pt/$FeO_x$ SACs exhibited a high atom utilization and unexpected catalytic activity, Pt SAzymes have attracted widespread attention.[123] A host of Pt SACs have been produced and widely used in a range of applications,[124] with $CeO_2$ being a unique support material.[125] For instance, Yan *et al.*[126] used Pt-$CeO_2$ SAzymes for the production of a new type of bandage for brain trauma. *In vitro* and *in vivo* experiments disclosed that the nanozyme-based bandage afforded sustained multienzyme activity (including POD-, CAT-, SOD-, and GPx-like activities), nontoxicity and excellent durability. The bandage significantly improved wound healing and reduced inflammation, which set a precedent for noninvasive therapy using SAzymes.

Liang *et al.* developed a practical strategy for engineering high-performance nanozymes by reversing the thermal sintering process, which atomized platinum nanoparticles into single atoms within a carbon matrix derived from ZIF-8 (Fig. 8a).[127] The P and S dopants not only promoted the atomization of Pt nanoparticles to $Pt_{TS}$-SAzyme, but also facilitated the formation of $Pt_1N_3PS$ active moieties due to electron donation of the P dopants and electron acceptance of the N and S dopants. The resultant $Pt_{TS}$ SAzyme was found to exhibit a remarkable POD-like activity by catalyzing the oxidation of POD substrates (*e.g.*, TMB, DAB, and OPD) to produce a color change (Fig. 8b). After thermal atomization of Pt nanoparticles into Pt single atoms, the POD-like catalytic activity and initial reaction velocity of $Pt_{TS}$-SAzyme were significantly higher than those of Pt nanoparticles or Pt-free N, P and S co-doped hollow carbon polyhedron (NPS-HC) (Fig. 8c and d). Pt SAzymes have also been prepared with Pt single atoms supported on g-$C_3N_4$ *via* a wet-chemistry strategy with alkali metal ions-intercalated g-$C_3N_4$ (g-$C_3N_4$-K) and a platinum salt precursor. The resulting SA-Pt/g-$C_3N_4$-K SAzyme remarkably enhanced the generation of $^{\bullet}OH$ radicals by reducing the desorption energy of the intermediate state of OH* from the active site during $H_2O_2$ activation.[128] This opens up a new way for the antibacterial application of Pt SAzymes.

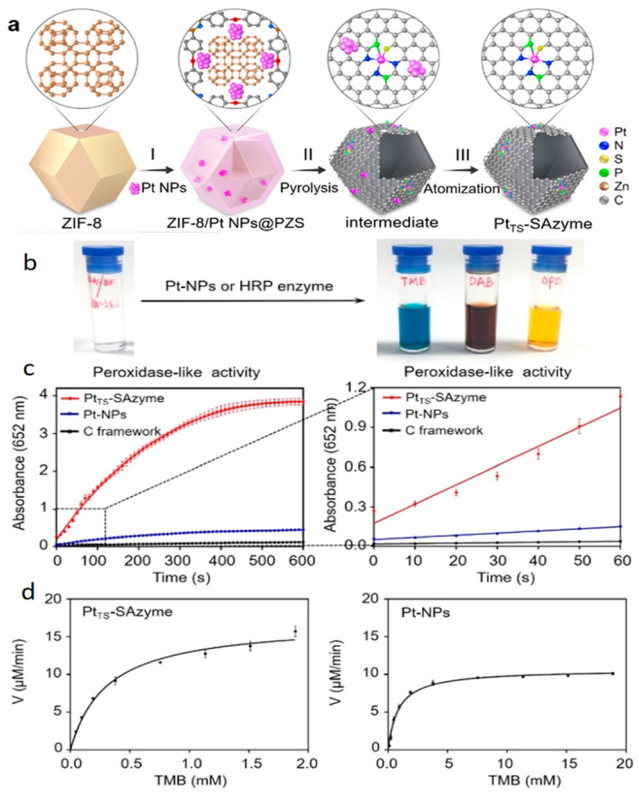


**Fig. 8** (a) Illustration of the preparation process of $Pt_{TS}$-SAzyme. (b) POD-like activity of Pt-based catalyzing the oxidation of POD substrates of TMB, DAB, and OPD to produce a color change. (c) (Left) Reaction–time curves of TMB oxidation catalyzed by PtTS-SAzyme, Pt-NPs nanozyme, or Pt-free inorganic C framework (NPS-HC); (right) zoom in of the initial linear portion of the reaction–time curves. (d) Reaction kinetics of (left) $Pt_{TS}$-SAzyme and (right) Pt-NPs nanozyme. Reproduced with permission from ref. 127, copyright 2021, American Chemical Society.

### 4.5 Other SAzymes

Other metals have also been used to prepare SAzymes. Among the metals with bactericidal effect, copper can effectively inhibit the growth of various harmful bacteria, viruses and microorganisms (such as algae) in water. However, as a heavy metal, the biological applications of copper and its compounds have remained limited due to metal toxicity.[129] The metal leaching effects can be minimized with Cu SAzymes. Zhu *et al.* observed that Cu SAzymes with Cu–N–C moieties exhibited intrinsic POD- and OXD-like activity to catalyze the generation of $^{\bullet}OH$ and $O_2^{\bullet-}$ from $H_2O_2$ and $O_2$, respectively.[130] The produced ROS displayed a significant activity towards the inhibition of bacterial growth. As the antibacterial activity of the Cu SAzymes was significantly superior to vancomycin, a common antibacterial drug (Fig. 9a), it is anticipated that Cu SAzymes will play a critical role in the development of new antibacterial agents and new antimicrobial strategies.

Song *et al.* observed an excellent phosphatase-like (PPA-like) activity with Ce–N–C SAzymes, which effectively catalyzed the dephosphorylation process of inorganic phosphate.[131] Notably, as $Al^{3+}$ could form Al–O bond *via* specific binding with O atom and inhibit the PPA-like activity (Fig. 9b), a fast, low-cost, portable, and efficient fluorescent liquid-phase sensor can be constructed for the sensitive detection of $Al^{3+}$.

Some other metals, such as Ru, Co, Au, and Se, have also been used as the active centers for SAzymes.[132] They are usually synthesized by wet chemistry and high-temperature pyrolysis. Notably, two different metal atoms can be combined to construct dual-atom structures, where the synergistic effects can be exploited for the manipulation of the electronic structure of the metal centers.[133] In earlier studies, these materials were mainly used as electrode catalysts for electrochemical energy technologies. In recent years, they have shown great potential in biomedical applications, such as tumor therapy and biosensing, with the continuous optimization of the structures and emergence of a variety of enzyme-like activities,[134] as demonstrated below in section 4.6.

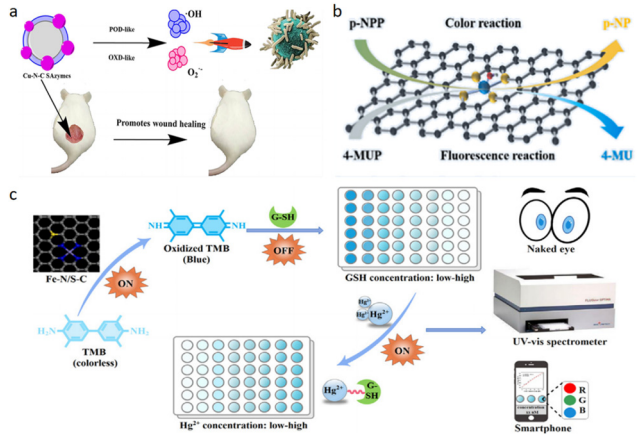


**Fig. 9** (a) Schematic diagram of the antibacterial activity of Cu–N–C SAzymes with intrinsic POD- and OXD-like activity. Reproduced with permission from ref. 130, copyright 2022, American Chemical Society. (b) Schematic diagram of the catalytic mechanism of Ce–N–C SAzyme with PPA-like activity for the rapid and sensitive detection of aluminum ions through color change and fluorescence signal generation during the catalytic process. Reproduced with permission from ref. 131, copyright 2022, Elsevier. (c) Schematic diagram of a colorimetric sensor based on Fe–N/S–C SAzymes for simultaneous multimode detection of GSH and $Hg^{2+}$. Reproduced with permission from ref. 137, copyright 2022, Elsevier.

### 4.6 Nonmetal dopants

For SAzymes, the M–N–C active moiety can be further engineered with the introduction of additional heteroatom dopants, such as O, S, and P, by taking advantage of their different electronegativity to manipulate the electronic property of the metal centers.[135] For instance, in comparison with the $FeN_4$ SAzyme and $Fe_3O_4$ nanozyme, $FeN_3P$ SAzyme by P doping into the Fe–N–C SAC exhibited markedly enhanced POD-like activity, as manifested in the colorimetric reaction of hydrogen peroxide and TMB.[136] DFT calculations showed that the adsorption energy of hydrogen peroxide was lowered to −0.40 eV on $FeN_3P$, as compared with −1.24 and −0.60 eV on $Fe_3O_4(111)$ and $FeN_4$, respectively, consistent with the enhanced kinetics of the dissociation of hydrogen peroxide into two surface OH species ($H_2O_2 \rightarrow 2OH$). Subsequently, in the $FeN_3P$ SAzyme, $FeN_4$ SAzyme and $Fe_3O_4(111)$ nanozyme, the two surface OH species reacted with each other to form surface O and $H_2O$ molecule ($2OH \rightarrow O + H_2O$) with an energy barrier of 0.49, 1.05 and 1.51 eV, respectively, which indicated that this process was most easily carried out on the surface of $FeN_3P$ SAzyme. However, since the $H_2O$ molecules were still adsorbed on the surface of the nanozyme, this could inhibit the catalytic process. A thermodynamic investigation was then conducted to examine the desorption of water molecules. The results showed that the desorption energy of water molecules was relatively low on the surface of all the three nanozymes under neutral conditions. In acidic media, the reaction potential energy of the transformation of OH species into $H_2O$ on $FeN_4$ SAzyme was increased to 2.84 eV, suggesting that OH would be stuck to the Fe centers and impede the catalytic process; by contrast, OH could be instantaneously converted into $H_2O$ on $Fe_3O_4(111)$, due to an ultralow reaction potential energy of 0.11 eV, which also led to failure of the catalytic process. Yet, the reaction potential energy of this process on $FeN_3P$ SAzyme was almost independent of solution pH, indicating that the surface OH species could be successfully converted into $H_2O$. The desorption of $H_2O$ can also occur easily due to a low barrier on the three nanozymes. In summary, the proposed reaction pathway demonstrated an enhanced catalytic activity of $FeN_3P$ SAzyme due to synergistic effects of the P dopants through the precise coordination to the metal centers. Similarly, Li *et al.*[137] introduced S dopants into Fe–N–C SAzyme, which not only manipulated the geometric configuration and electronic structure of the metal centers, but also reduced the formation of inactive Fe carbide, and facilitated the formation of a porous carbon structure with a high specific surface area. The resulting Fe–N/S–C SAzyme exhibited enhanced OXD-mimicking activity due to the auxiliary regulation of the S atoms, as compared with the Fe–N–C counterparts (Fig. 9c).

Doping of polynary metals has also been employed to construct SAzymes with a high density of activity sites, where the addition of multiple metals can form active sites and regulate the electronic structure through the interactions between the metal centers.[138] Therefore, the binding energy of reactants, intermediates, and products can be modulated for an optimal catalytic performance. In a recent study,[139] a Fe–Bi bimetallic SAzyme (Fe/Bi-NC) was prepared by using Fe-doped Bi-MOF as the precursor, and consisted of $Fe–N_4$ and $Bi–N_4$ dual-sites. The role of Fe was not only to generate active sites, but also to expand the distance of neighboring Bi atoms and prevent their aggregation. Meanwhile, PVP surfactants were added to prevent the interlayer accumulation of the MOF precursor through chemical adsorption. During pyrolysis the precursor was transformed into thin-sheet Fe/Bi-NC, a unique structure conducive to the formation of single-atom sites. Experimental studies and DFT calculations confirmed the positive synergistic effect between the $FeN_4$ and $BiN_4$ sites, which markedly enhanced the OXD-like activity. Yet, an Fe content over 4% actually diminished the enzymatic activity. Therefore, accurate regulation of the contents of constituent atoms is critical for attaining ideal bimetallic SAzymes. In another study, Au–Ni/g-$C_3N_4$ SAzymes were produced with g-$C_3N_4$ nanosheets doped with Au–Ni bimetallic nanoparticles,[140] which exhibited apparent POD-like activity and could be used for the colorimetric detection of glucose. In enzyme kinetics measurements, the $K_m$ values were found to be lower with the bimetal SAzymes than those of their monometallic counterparts, indicating enhanced affinity of the Au–Ni/g-$C_3N_4$ nanocomposite toward the substrates. In fact, the enhanced catalytic activity was attributed to the synergistic effects between the Au and Ni atoms. Due to a clear difference of the ionization potential between Au and Ni (9.22 eV and 7.63 eV), electron transfer occurred from Ni to Au, resulting in an increase in the charge density of Au, such that both Au and Ni could act as active sites for the POD-like activity. This bimetallic synergistic effect has also been previously reported in the literature.[141]

In summary, one can see that metal centers are the active sites that dictate the catalytic activity of SAzymes, due to the formation of unique M–N–C coordination structures.[103] For instance, among the Fe-based SAzymes, the $FeN_3$ moiety is known to exhibit a strong OXD-like catalytic activity because $O_2$ molecules adsorb readily onto the $FeN_3$ centers *via* a side-on configuration, which is the first step in the OXD-like reaction and plays an important role in the subsequent steps.[142] $FeN_4$ SAzymes, however, usually exhibit excellent POD-like activity, because the $FeN_4$ active sites mimic the porphyrin iron cofactor structures (Fe atoms coordinated to four nitrogen atoms in the plane of the porphyrin ring) of natural HRP.[36] For $FeN_5$ SAzymes, the electronic structure of the Fe centers is optimized due to the addition of the axial ligand through the nitrogen atom, which facilitates the electron-transfer kinetics and leads to a better OXD- and POD-like activity than that of $FeN_3$ and $FeN_4$.[55]

Similarly, with a zinc-centered porphyrin-like structure, Zn-based SAzymes also display outstanding POD-like activity. The unsaturated-coordination $ZnN_4$ centers can catalyze the decomposition of $H_2O_2$ into $^{\bullet}OH$, which is similar to the catalytic pathway of HRP.[143] Cu-based SAzymes not only exhibit OXD- and POD-like activity but also mimic polyphenol oxidase (*e.g.*, tyrosinase, catechol oxidase, and laccase), where the active sites all feature coupled multinuclear Cu(II) centers and can oxidize important biological substrates (*e.g.*, polyphenols and polyamines) and directly activate oxygen.[144]

Notably, these enzymatic activities are sensitively dependent on solution pH. Under different pH conditions with different metal centers, $H_2O_2$ can be decomposed into different forms. Specifically, SAzymes typically exhibit POD-like activity at low pH and CAT-like activity at high pH.[145] The number of coordinating nitrogens can also impact the catalytic activity. For example, when the number ($x$) of coordinating N in $CoN_x$ decreases from 4 to 2, Co SAzymes show an enhanced activity towards oxygen reduction reaction,[146] while $FeN_5$ SAzymes display a better OXD- and POD-like activity than both $FeN_4$ and $FeN_3$.

Therefore, to improve and optimize the catalytic performance of SAzymes, the elemental composition, metal coordination configuration, metal loading and supports interactions need to be systematically varied and carefully examined,[104] as they affect the geometric configuration and electronic structure of the metal centers, resulting in different catalytic activity and selectivity. This is of particular importance for SAzymes that possess multi-enzyme activity and find diverse applications in antibacterial, cancer therapy, and cell protection.[147]

## 5. Biological and medical applications

### 5.1 Biosensing

Due to their low cost, high efficiency, high sensitivity and great stability, SAzymes have been successfully utilized in the construction of a variety of biosensors based on colorimetric, electrochemical and fluorescence platforms.[148] Most colorimetric biosensors are based on the TMB redox chemistry, as TMB can be oxidized to a blue product (oxTMB) catalyzed by the POD-like activity of SAzymes, which can be readily detected with an absorption peak at 652 nm, and the concentration of the target analyte can be determined from the absorbance.[149] For instance, Zhou *et al.*[150] fabricated an Fe SAzyme by an isolation–pyrolysis procedure which displayed POD-like activity and catalyzed the oxidation of TMB in the presence of $H_2O_2$ generated from the oxidation of galactose with galactose oxidase (Gal Ox) (Fig. 10a). The colorimetric sensor exhibited a good linear relationship between the optical absorbance and galactose concentration, with a good minimum detection limit, which paved the way for a rapid and economical detection of galactose and diagnosis of galactosemia. Similarly, in a Bi SAzyme anchored onto Au hydrogels (BiSA@Au),[151] the Bi atoms and the unique porous nanowire networks of the hydrogels greatly improved the catalytic activity by decreasing the potential barriers for the decomposition of $H_2O_2$. With the immobilization of GOx on the surface of the BiSA@Au nanozyme, the oxidation of TMB could be exploited for the accurate and sensitive colorimetric detection of glucose in clinical

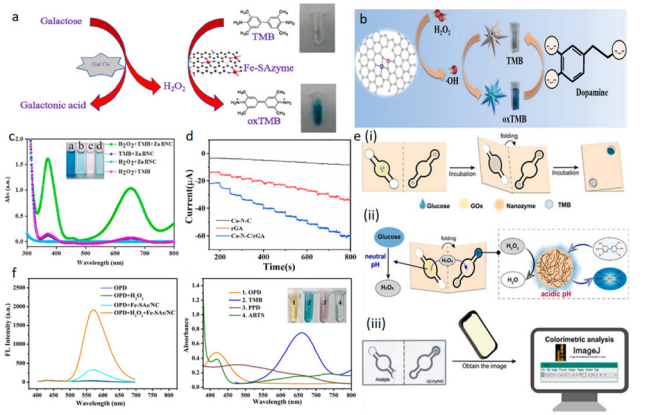


**Fig. 10** (a) Schematic illustration of the colorimetric assay for galactose detection by an Fe SAzyme. Reproduced with permission from ref. 150, copyright 2020, Elsevier. (b) Schematic illustration of dopamine determination by $FeN_3/PtN_4$ dual-site SAzymes. Reproduced with permission from ref. 152, copyright 2022, Springer. (c) UV–vis spectra of ZnBNC, ZnNC and $H_3BO_3$–ZnNC in the $H_2O_2$/TMB solution. Inset is the photograph of the various solution. Reproduced with permission from ref. 153, copyright 2020, Elsevier. (d) Amperometric response of Co–N–C, rGA and Co–N–C/rGA on a GCE with the addition of 100 μM $H_2O_2$ in 0.01 M PBS (pH 7.4). Reproduced with permission from ref. 156, copyright 2023, Elsevier. (e) Schematic illustration of the colorimetric detection of glucose *via* PGA-Fe/CS NPs-incorporated foldable paper microfluidic device (PGA-Fe/CS@FμPAD). (i) Glucose detection procedure, (ii) cascade reaction incorporating glucose oxidation under neutral pH and $H_2O_2$ reduction with TMB oxidation under acidic pH, and (iii) on-site quantification *via* an image acquired with a smartphone. Reproduced with permission from ref. 157, copyright 2023, Elsevier. (f) (Left) Fluorescence emission spectra of OPD, OPD/$H_2O_2$, OPD/Fe-SAs/NC, and OPD/$H_2O_2$/Fe-SAs/NC, and (right) UV-vis absorption spectra of $H_2O_2$/Fe-SAs/NC with the substrates of OPD, TMB, PPD and ABTS. Inset is the photograph of the various solutions. Reproduced with permission from ref. 160, copyright 2020, Elsevier.

samples. In another study with $FeN_3/PtN_4$ dual-atom SAzymes,[152] a colorimetric sensing platform was obtained for the quantization of dopamine whereby the POD-like activity of $FeN_3/PtN_4$ was utilized to catalyze the oxidation of TMB by $H_2O_2$ to generate blue oxTMB, and then the addition of dopamine reduced oxTMB back to colorless TMB (Fig. 10b). Similarly, Feng *et al.* synthesized B-doped Zn–N–C (ZnBNC) SAzymes for the colorimetric detection of *p*-phenylenediamine (PPD), a reductive carcinogen,[153] which reduced blue oxTMB to colorless TMB, with a linear decrease of the absorbance with PPD concentration (Fig. 10c).

Notably, the oxidation of TMB can be inhibited by a range of small-molecule compounds that are effective indicators of human health, such as uric acid, dopamine, norepinephrine and ascorbic acid. This unique chemistry can be exploited for the development of biosensors for their indirect detection.[114] For instance, Wu *et al.* prepared an Fe SAzyme with a high OXD-like activity at pH 3.0, and the activity could be effectively inhibited by 4-acetamidophenol (AMP) *via* a reversible mixed-inhibition mechanism.[154] This unique property could be exploited for the detection of AMP.

In electrochemical biosensing, Hu *et al.*[155] prepared an A-Co-NG SAzyme with Co atomically dispersed into N-doped graphene for electrochemical detection of uric acid by measuring the change of the current signals involved in the oxidization of uric acid molecules. Liu *et al.*[156] optimized the Co–N–C structure of a Co SAzyme by embedding Co atoms into a reduced graphene oxide aerogel (rGA) forming a three-dimensional layered electrochemical electrode, which exhibited a high electrocatalytic performance in the *in situ* detection of $H_2O_2$, uric acid and dopamine. By monitoring the current response of Co–N–C, rGA and Co–N–C/rGA on a glassy carbon electrode (GCE) under different experimental parameters, it was found that Co–N–C/rGA exhibited the best catalytic performance among the series (Fig. 10d).

Notably, POD-mimicking nanozymes require an acidic medium to exhibit the enzymatic activity, while near-neutral pH is the optimal condition for GOx. The cumbersome steps of switching pH during the sensing operation bring tremendous obstacles to the cascade reaction of the two enzymes. To mitigate these issues, a foldable paper microfluidic device has been rationally designed which is divided into two parts at acidic and neutral pH for the Fe SAzymes and GOx, respectively (Fig. 10e(i)).[157] Experimentally, glucose is oxidized by GOx under neutral pH generating $H_2O_2$, which then migrates to the other compartment by folding the paper device, producing a colorimetric signal under acidic pH (Fig. 10e(ii)). The unique technology breaks the pH restriction of cascade reactions and may serve as an innovative portable integrated microdevice for rapid detection of glucose, a key step in the further development of point-of-care testing (POCT) (Fig. 10e(iii)). In fact, a range of biosensors are being developed within the context of miniaturization, integration and wearability. The devices are portable, exhibit a fast detection speed, and can be integrated with artificial intelligence and informational technology for remote, real-time monitoring. Nevertheless, there are not many examples of SAzymes used in these applications yet. It is anticipated that the construction of stable POCT devices with SAzymes instead of natural enzymes will greatly extend the sensor lifetime. Improving the stretchability of SAzymes through rational design to build wearable biosensing devices will also create an emerging pathway.[158]

Furthermore, fluorescence-based biosensors have also been fabricated with SAzyemes.[159] For instance, Wang *et al.*[160] utilized the POD-like activity of Fe SAzymes to catalyze the oxidation of nonfluorescent OPD to fluorescent DAP, with a maximum fluorescence emission peak at 566 nm. The generated DAP efficiently quenched the fluorescence emission of polyvinylpyrrolidone-protected copper nanoclusters (PVP-CuNCs) at 438 nm; yet this could be blocked by thiocholine derived from acetylthiocholine by acetylcholinesterase (AChE). Therefore, the ratio of the fluorescence emission at 566 and 438 nm ($F_{566}/F_{438}$) could be exploited for the quantification of the AChE activity (Fig. 10f).

In addition to the above-mentioned biosensors, nanozyme-based immunosensors have also been reported. In a typical sandwich-type immunosensor, the target (antigen) first binds to the corresponding specific antibody, followed by the neuraminidase (NANase)-linked antibody, which then binds to the recognized antigen, thus forming a sandwich structure. For SAzyme-based immunosensors, the optimized electronic structure can lead to a high catalytic activity. The introduction of SAzymes catalyzes some chromogenic reactions, which to some extent compensates for the lack of sensitivity of colorimetric analysis, while maintaining a good activity after prolonged storage within a wide range of pH and temperature.[161]

Furthermore, the accurate detection of DNA usually requires a combination of signal amplification strategies by, for instance, nanozymes. However, the use of SAzymes for this purpose has been relatively rare. It can be envisaged that when a DNA probe is modified with SAzymes that can catalyze the chromogenic reaction of the relevant chromogenic substrate, precise detection of DNA can be achieved in conjunction with a signal amplification strategy.[162]

### 5.2 Cancer diagnosis and therapy

SAzymes featuring various enzyme-like activities have also been creatively introduced to assist the diagnosis and treatment of cancers, which is efficient, non-toxic, biocompatible, and non-invasive (Fig. 11).[163,164] Ferroptosis is a cell death mechanism discovered in 2012. It is caused by the accumulation of iron-dependent lipid peroxidization (LPO), which induces lethal disruption of the cell membrane structure. Glutathione peroxidase 4 (GPx-4) can reduce the production of LPO by taking GSH as a cofactor, but glutathione oxidase (GSHOx) will promote the conversion of GSH to glutathione disulfide (GSSG), resulting in the deactivation of GPx-4 and thus increasing the accumulation of LPO. In 2021, Lin's group reported an innovative strategy of mild photothermal therapy (PTT) based on Pd SAzymes to promote the treatment of ferroptosis.[165] The Pd SAzyme showed POD- and GSHOx-like activities and photothermal conversion performance, which

 

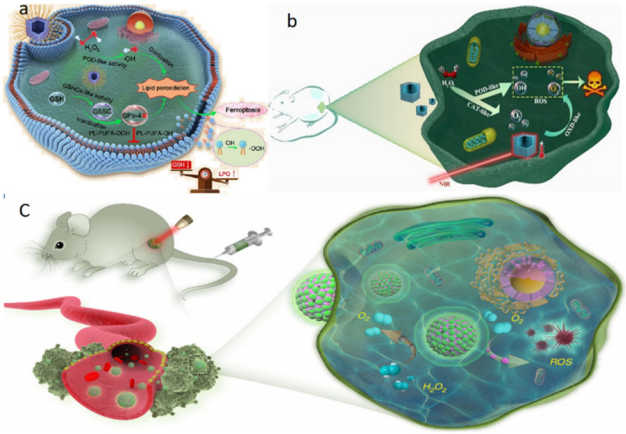


**Fig. 11** (a) Illustration of inhibiting tumor cell growth by inducing iron ferroptosis. Sulfurized S–N/Ni PSAE exhibits higher GSHOx-like activity than nitrogen-monodoped N/Ni PSAE for depleting intracellular GSH, resulting in the inactivation of GPx-4. Moreover, S–N/Ni PSAE with superior POD-like activity converts endogenous $H_2O_2$ into highly toxic $^{\bullet}OH$, causing LPO *via* oxidizing PUFAs. Reproduced with permission from ref. 167, copyright 2023, American Chemical Society. (b) Illustration of manganese-based single-atom enzyme for tumor therapy utilizing the synergetic catalytic and photothermal therapy. Reproduced with permission from ref. 171, copyright 2021, Wiley. (c) Scheme of continuously catalytic oxygen generation and ROS production for enhanced tumor photodynamic therapy by OxgeMCC-r SAzyme. Reproduced with permission from ref. 164, copyright 2020, Springer Nature.

could lead to the up-regulation of LPO and ROS. The accumulation of LPO and ROS provided a powerful way to split heat shock proteins (HSPs) which could repair cell damage caused by heat, making Pd SAzyme-mediated mild PTT possible.

In 2022, considering the effects of hyperthermia on the activity of SAzymes and the damage of cell tissue, Liu's group used $Bi_2Fe_4O_9$ nanosheets as an enzyme mimic by low-temperature activation (4–37 °C), which featured a wider safety window than those treated at higher temperatures (37–42 °C). The cold-activated SAzyme displayed GSHOx- and POD-like activity and mediated the antitumor treatment.[166] Notably, the GSHOx-like activity of the $Bi_2Fe_4O_9$ SAzyme could only be activated at low temperatures, whereas the POD-like activity of $Bi_2Fe_4O_9$ SAzyme in acidic media and the CAT-mimic activity in neutral and alkaline conditions were unaffected by temperature changes. Therefore, the GSHOx-like activity activated at low temperatures promoted the oxidation of GSH to generate $H_2O_2$. Then intrinsic $H_2O_2$ together with the $H_2O_2$ generated from GSH oxidation was decomposed by POD-like $Bi_2Fe_4O_9$ SAzymes. When the GSHOx-like activity was turned off by an interventional device (*e.g.*, a smart phone), the enzyme activity could be remotely and precisely modulated, so as to eliminate excessive ROS through CAT-like activity and minimize damage to normal tissues. Similarly, Wu's group observed that a Ni SAzyme doped with sulfur and nitrogen *via* an anion exchange method showed better POD- and GSHOx-like activity than its undoped counterparts and could effectively inhibit the growth of tumor cells without toxicity (Fig. 11a).[167]

As the tumor microenvironment features insufficient oxygen supply and excessive ROS (such as $H_2O_2$),[168] one can take advantage of the unique activity of SAzymes to catalyze the decomposition of $H_2O_2$ to cytotoxic hydroxyl radicals ($^{\bullet}OH$) and locally kill the tumor cells. This was indeed demonstrated recently by He *et al.* with a Pd SAzyme based on phenolic carbon quantum dot (DA-CQD@Pd).[169] Meanwhile, SAzymes can catalyze free-radical polymerization to form immune adjuvant CpG oligodeoxynucleotides (ODN), which can initiate catalytic immunotherapy to achieve localized immunomodulation and prevent tumor metastasis. Liu's group prepared an Fe SAzyme containing $FeN_5$ moieties embedded within N-rich carbon *via* a melamine-mediated two-step pyrolysis strategy,[55] where the $FeN_5$ active sites catalyzed the decomposition of $H_2O_2$ to $^{\bullet}OH$. Feng's group integrated Au nanoparticles into the pores of a dendritic mesoporous Fe SAzyme,[170] where the Au nanoparticles interacted with glucose to generate gluconic acid and $H_2O_2$ in a nanozyme-like manner, and $H_2O_2$ was further decomposed into ROS due to the POD-like activity of the Fe SAzyme. This kind of POD-like activity can cut off the energy supply of the tumor cells, and in combination with photothermal agents (PTAs), achieve photothermal treatment of tumors at low temperatures.

Apart from the POD-like activity, many SAzymes possess multienzyme properties and can initiate cascade enzymatic reactions and enhance therapeutic efficacy. Zhu *et al.* utilized hollow ZIF as a precursor to prepare a PEGylated manganese-based SAzyme (Mn/PSAE), which catalyzed the conversion of cellular $H_2O_2$ to $^{\bullet}OH$ by POD-like activity, as well as promoted the production of $O_2$ from $H_2O_2$ and the conversion of $O_2$ to $O_2^{\bullet-}$ *via* OXD-like activity.[171] The amorphous carbon substrate materials could enhance the PTT effect. In short, the enzyme cascade reactions initiated by SAzymes with multienzyme catalytic properties facilitate the continuous redox reaction of cells and the accumulation of cytotoxic ROS, which is a favorable and implementable pathway to enhance the anti-tumor effect (Fig. 11b).

Despite such breakthroughs in SAzyme-based tumor therapy, there remains much room to improve the specificity. Studies have shown that the combination of nanomotor and near-infrared (NIR) technology can enhance the adhesion of SAzymes to the cancer cell membrane and deepen penetration into the tumor.[172] Another desirable route is to combine chemodynamic therapy,[173] sonodynamic therapy[174] and photothermodynamic therapy[175] to improve targeting. One can envision that precise drug administration can be achieved when drugs are loaded onto the SAzymes for targeted transport to the cancer sites.[176] In conclusion, targeted tumor therapy has remained a key clinical challenge, and SAzymes have emerged as a unique platform, which demands further and more thorough studies.

### 5.3 Antibacterial and antiviral activity

Bacterial infection is a grave threat to human health, which is compounded by the emergence of drug-resistant bacteria. ROS can act as powerful weapons against pathogen invasion by dis-

integrating the structure of biofilms, while avoiding the generation of drug-resistant strains through the effective damage of bacterial cells.[177,178] SAzymes possess unique advantages as compared with traditional antibacterial agents, such as high efficiency, low cost, good biocompatibility, non-cytotoxicity and adjustable enzyme activity, where the bactericidal mechanism is primarily based on *in vivo* decomposition of hydrogen peroxide or oxygen to ROS.[179]

Previous reports have shown that Cu SAzyme exhibited excellent antibacterial activity. Zhao *et al.* prepared a highly accessible Cu SAC supported on biocompatible N-doped mesoporous carbon nanospheres *via* an emulsion-template method.[180] The ultra-large pore size and small particle size of the mesoporous carbon nanospheres boosted the efficient conversion of $O_2$ to $O_2^{\bullet-}$, resulting in damage to the bacterial cell membrane and the splitting of the bacterial body. Wang *et al.* synthesized N-doped porous carbon-supported Cu SAzymes (Cu SASs/NPC) by a pyrolysis–etching–adsorption–pyrolysis (PEAP) strategy.[181] The Cu SAzymes possessed prominent POD-like activity in catalyzing the decomposition of $H_2O_2$ to $^{\bullet}OH$ and GSH peroxidase (GSH-Px)-like activity to deplete GSH, and consequently a nearly 100% antibacterial efficacy against the two most common pathogenic bacteria, *Escherichia coli* (*E. coli*) and methicillin-resistant *Staphylococcus aureus* (*S. aureus*) through the synergistic effect of PTT (Fig. 12a). Meng *et al.* utilized a unique support consisting of a nanodiamond core and curved graphene shells (ND@G) that was decorated with abundant defects to anchor Cu metal atoms, resulting in atomically dispersed and fully exposed $Cu_3$ clusters on the ND@G surface (Fig. 12b).[182] This structure significantly enhanced the OXD-like activity in the dissociation of $O_2$ into $^{\bullet}OH$ to kill bacteria.

In addition to copper, other metal SAzymes also show effective antibacterial activity. Yang's group prepared a g-$ZnN_4$-$MoS_2$ SAzyme *via* electrostatic interactions which can be applied to sonodynamic ion therapy to upgrade the antibacterial efficacy.[183] Benefiting from the synergetic regulation of the Zn single-atom and $MoS_2$ quantum dots, charge transfer and spin–flip were enhanced at the heterogeneous interfaces, which promoted the generation of singlet $^1O_2$ from $O_2$ owing to a reduced activation energy of $O_2$. It has been shown that $^1O_2$ can kill *S. aureus* with an antibacterial efficiency of 99.58% under 20 min of ultrasound irradiation. The excellent sonodynamic antibacterial efficiency and osteoinduction ability of g-$ZnN_4$-$MoS_2$ suggested attractive ultrasonic antimicrobial applications. Another similar instance is a Pt SAzyme-modified porphyrin MOF (PCN-222-Pt), where the active sites exhibit strong OXD- and POD-like activities and can lower the desorption energy of $O_2$ and produce ROS (Fig. 12c). It displays an excellent anti-biofilm performance to deactivate bacteria, with an inactivation efficiency in *S. aureus* and *E. coli* of 98.69% and 99.91%, respectively.[184]

SAzymes possess not only prominent bactericidal activity, but also play a vital role as high-efficiency catalysts in antiviral research. Notably, Wang *et al.*[185] prepared Ag-$TiO_2$ SAzymes to combat SARS-$CoV_2$ coronavirus, which is currently posing a serious threat to global public health. The materials were

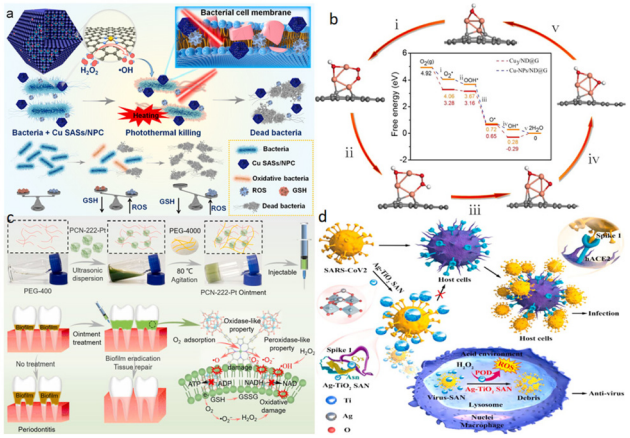


**Fig. 12** (a) Cu SASs/NPC with GSH-depleting performance for photothermal-catalytic therapy against bacteria. Cu SASs/NPC as GSH-like mimetic enzyme and HRP-like nanozyme for eradicating *E. coli* and *MRSA in vitro*. Reproduced with permission from ref. 181, copyright 2021, Elsevier. (b) Theoretical investigation of OXD-like activity over Cu-NPs/ND@G and $Cu_3$/ND@G. The optimized adsorption configurations of various intermediates along the oxidase-like reaction path on $Cu_3$/ND@G and the free energy diagram for the oxidase-like mechanism on $Cu_3$/ND@G and Cu-NPs/ND@G. The gray, brown, red and white balls represent C, Cu, O, and H atoms, respectively. Reproduced with permission from ref. 182, copyright 2022, Elsevier. (c) Preparation of the injectable HNTM-Pt ointment with enzyme-like catalytic activities and the treatment of periodontitis through a series of catalytic reactions. Reproduced with permission from ref. 184, copyright 2022, Elsevier. (d) Schematic of Ag-$TiO_2$ SAzymes with anti-SARS-$CoV_2$ activity. Ag-$TiO_2$ SAzymes adsorb onto the receptor binding domain (RBD) of spike 1 protein of SARS-$CoV_2$ containing abundant cysteine and asparagine to generate the SAzyme/virus complex, which can be phagocytosed by macrophages and colocalized with lysosomes. Reproduced with permission from ref. 185, copyright 2021, Elsevier.

rationally designed through a combination of ingenious experimental engineering and theoretical calculations, and exhibited a high POD-like activity (Fig. 12d). Scanning electron microscopy (SEM) measurements showed that the SAzyme adsorbed onto the receptor binding domain (RBD) of the spike 1 protein of SARS-$CoV_2$ that contained abundant cysteine and asparagine *via* strong interactions with the Ag centers. The SAzymne/virus complex was then phagocytosed by macrophages and colocalized with lysosomes which supplied an appropriate acid condition for enzyme activity. Compared with traditional $TiO_2$ or Ag nanomaterial, Ag-$TiO_2$ SAZyme exhibited a much higher adsorption efficacy (99.65%) of SARS-$CoV_2$ pseudovirus. This demonstrated the great potential of SAzymes in antiviral applications.

### 5.4 Other applications

SAzymes have also been successfully applied in food safety monitoring,[186–189] environmental survey,[190–193] cytoprotection,[194,195] wound healing,[196] nervous system diseases therapy and brain trauma,[197–200] as well as drug dosing guides and outcome predictions. For instance, Ce–N–C SAzymes have been utilized for food safety monitoring and

detection of pesticide residues, where the POD-like activity provided a colorimetric route to the efficient detection of organophosphorus and carbamate pesticide residues *via* cascade reactions with AChE. The Ce SAzyme was integrated with bioactive paper using the 3D printing technology.[201] Mechanistically, TMB were oxidized to blue oxTMB, which was then reduced to colorless TMB by choline in the presence of Ce–N–C SAzyme and hydrogen peroxide. However, organophosphorus and carbamate pesticide residues could inhibit the activity of AChE and produce little or no choline, blocking the reverse reduction reaction. The color of bioactive paper was correlated with the pesticide residue content, allowing for the rapid portable detection of pesticides. Furthermore, Yang's group found that hemin-loaded Zn–N–C SAzymes possessed an intrinsic POD-like activity, which could be used for rapid detection of propylgallate and formaldehyde in food samples.[202] The POD-like activity led to the oxidation of colorless propylgallate to yellow products while HCHO could inhibit propylgallate oxidation, leading to an apparent decrease in optical absorbance.

In addition, SAzymes exhibit antibacterial activity against a broad range of marine microorganisms and can act as promising anti-biofouling agents. Sun *et al.* developed a Co SAzyme with Co single atoms loaded into polyacrylamidoxime (PAO).[203] The Co-PAO SAzyme catalyzed the generation of ROS from hydrogen peroxide and destruction of marine fouling biological entities, such as marine bacteria and marine algae.

Furthermore, the abundant ROS generated by oxidative stress can damage brain tissue and induce a series of neuroinflammation events, leading to the occurrence of various central nervous system (CNS) diseases; select SAzymes have been found to exhibit satisfactory ROS-scavenging activity and great potential for the treatment of CNS diseases.[204] For instance, ultrasmall carbon dots-supported Fe SAzyme (Fe-CDs) could serve as a kind of nontoxic nanomedicine to modulate the tumor microenvironment *via* ROS regulation and lysosome-mediated autophagy.[205] It has six naturally occurring enzymatic properties, OXD, CAT, SOD, and the POD family (HRP, GPx, and thiol peroxidase), that induce a cascade of reactions *in vivo*. In addition, blood–brain barrier permeability and the ability to selectively target glioblastoma (GBM) *in vivo* can be greatly enhanced by peptide modification on the surface of Fe-CDs. Benefiting from multiple enzyme-mimicking properties and minimal toxicity, the Fe-CDs SAzymes possess great potential for the precise therapy of drug-resistant GBM. Recently, Zhang *et al.* observed an ultrahigh biological activity of $RhN_4$, $VN_4$, and $FeCuN_6$ SAzymes through precise atomic engineering. The $RhN_4$ and $VN_4$ SAzymes formed an Rh/V–O–$N_4$ active site, displaying 4- and 5-fold higher affinity in POD-like performance than the $FeN_4$ and natural HRP. The $RhN_4$ structure also showed a CAT-like activity that was 20 times higher than that of the natural enzyme, while the $VN_4$ structure possessed a high GPx-like activity 7 times higher than that of the natural counterpart. The $FeCuN_6$ also showed excellent SOD-like activity. These catalytic activities can be combined to construct novel healing sutures for brain trauma by promoting the vascular endothelial growth factor, regulating the immune cells like macrophages, and reducing inflammation.[206]

## 6. Conclusion and perspectives

SAzymes are a rising star in the field of catalysis and biomedicine, primarily because of multiple catalytic activities that mimic those of POD, OXD, CAT, and SOD, which can mediate the redox reactions between various substances, generating or scavenging ROS. In comparison with the easy degradation and high costs of natural enzymes and complicated structures and limited catalytic activity of conventional nanoparticle-based nanozymes, SAzymes possesses excellent stability, well-defined central structure and low cost, leading to diverse applications in various fields. With the homogeneously dispersed active sites and well-defined coordination structures of SAzymes, it has become possible to explore the correlation between the material structure and activity *via* rational regulation of the geometric and electronic structure. As highlighted in this review, there is no doubt that SAzymes, as emerging high-performance biocatalysts, will become promising alternatives to traditional enzymes for a range of biological/biomedical applications.

Yet, despite significant progress, obstacles and challenges remain that hinder the further development of SAzymes. From the materials perspectives, most SAzymes are prepared by controlled pyrolysis of select precursors, where the carbon scaffolds typically exhibit a complex structure and aggregation of metal atoms inevitably occurs. The complexity of the material structure makes it challenging to establish an unambiguous correlation between the material structure and enzymatic activity. Thus, the development of effective methods for the preparation of SAzymes with well-defined structures is urgently needed. This calls for careful design of the precursors as well as deliberate manipulation of the thermal treatment conditions. Towards this end, ultrafast synthesis may be a viable option, where ultrashort heating pulses can facilitate the retention of the organized structures of the precursors.[207] In addition, one may take advantage of the latest breakthroughs in organometallic chemistry to pre-position the metal centers within a molecular framework.[208] This will also be of particular importance when binuclear or even multinuclear atomic sites are desired.

From the biological perspective, while enzyme-like activities have been observed with SAzymes, the catalytic performance and substrate selectivity have remained mostly subpar as compared with natural enzymes. This is likely due to the high-order structure of the nanocomposites that deviates from the natural enzyme. With advances in computing power and methods, the material structure of the nanocomposite-based SAzymes can be optimized within the context of, for instance, covalency between the metal center and coordinating atoms, porosity of the structural scaffold, doping of heteroatoms, *etc*.

In addition, thus far, mechanistic insights into the interactions between SAzymes and biological targets have remained

limited. This is particularly true with living microorganisms like bacterial cells and viruses, where the antimicrobial and antiviral activity may be a combined contribution of damage to cell structural integrity and inhibition of metabolism. *In vivo* imaging and spectroscopy analysis will be a key to unravelling the mechanistic details, which can be aided by low-temperature electron microscopy measurements.[209,210]

## Author contributions

Xueqian Xiao: investigation, writing – original draft; Xiao Hu: investigation, writing – original draft; Qiming Liu: writing – review & editing; Yulin Zhang: writing – original draft; Guo-Jun Zhang: resources, writing – original draft; Shaowei Chen: conceptualization, resources, writing – review & editing.

## Conflicts of interest

There are no conflicts to declare.

## Acknowledgements

This work was supported, in part, by the National Science Foundation (CBET-1848841, CHE-1900235, and CHE-2003685).

## References

1 J. Bjerre, C. Rousseau, L. Marinescu and M. Bols, Artificial enzymes, "chemzymes": current state and perspectives, *Appl. Microbiol. Biotechnol.*, 2008, **81**, 1–11.
2 J. Wu, X. Wang, Q. Wang, Z. Lou, S. Li, Y. Zhu, L. Qin and H. Wei, Nanomaterials with enzyme-like characteristics (nanozymes): next-generation artificial enzymes (II), *Chem. Soc. Rev.*, 2019, **48**, 1004–1076.
3 L. Gao, J. Zhuang, L. Nie, J. Zhang, Y. Zhang, N. Gu, T. Wang, J. Feng, D. Yang, S. Perrett and X. Yan, Intrinsic peroxidase-like activity of ferromagnetic nanoparticles, *Nat. Nanotechnol.*, 2007, **2**, 577–583.
4 F. Pogacean, C. Socaci, S. Pruneanu, A. R. Biris, M. Coros, L. Magerusan, G. Katona, R. Turcu and G. Borodi, Graphene based nanomaterials as chemical sensors for hydrogen peroxide – A comparison study of their intrinsic peroxidase catalytic behavior, *Sens. Actuators, B*, 2015, **213**, 474–483.
5 R. Ragg, M. N. Tahir and W. Tremel, Solids Go Bio: Inorganic Nanoparticles as Enzyme Mimics, *Eur. J. Inorg. Chem.*, 2015, **2016**, 1906–1915.
6 L. Gao and X. Yan, Nanozymes: an emerging field bridging nanotechnology and biology, *Sci. China: Life Sci.*, 2016, **59**, 400–402.
7 H. Wei and E. Wang, Nanomaterials with enzyme-like characteristics (nanozymes): next-generation artificial enzymes, *Chem. Soc. Rev.*, 2013, **42**, 6060–6093.
8 Y. Lin, J. Ren and X. Qu, Catalytically active nanomaterials: a promising candidate for artificial enzymes, *Acc. Chem. Res.*, 2014, **47**, 1097–1105.
9 Y. Ai, Z. N. Hu, X. Liang, H. B. Sun, H. Xin and Q. Liang, Recent Advances in Nanozymes: From Matters to Bioapplications, *Adv. Funct. Mater.*, 2021, **32**, 2110432.
10 A. P. Periasamy, P. Roy, W.-P. Wu, Y.-H. Huang and H.-T. Chang, Glucose Oxidase and Horseradish Peroxidase Like Activities of Cuprous Oxide/Polypyrrole Composites, *Electrochim. Acta*, 2016, **215**, 253–260.
11 D. Jiang, D. Ni, Z. T. Rosenkrans, P. Huang, X. Yan and W. Cai, Nanozyme: new horizons for responsive biomedical applications, *Chem. Soc. Rev.*, 2019, **48**, 3683–3704.
12 Y. Zhang, Y. Jin, H. Cui, X. Yan and K. Fan, Nanozyme-based catalytic theranostics, *RSC Adv.*, 2019, **10**, 10–20.
13 M. Liang and X. Yan, Nanozymes: From New Concepts, Mechanisms, and Standards to Applications, *Acc. Chem. Res.*, 2019, **52**, 2190–2200.
14 J. Han and J. Yoon, Supramolecular Nanozyme-Based Cancer Catalytic Therapy, *ACS Appl. Bio Mater.*, 2020, **3**, 7344–7351.
15 C. Hong, X. Meng, J. He, K. Fan and X. Yan, Nanozyme: A promising tool from clinical diagnosis and environmental monitoring to wastewater treatment, *Particuology*, 2022, **71**, 90–107.
16 L. Jiao, H. Yan, Y. Wu, W. Gu, C. Zhu, D. Du and Y. Lin, When Nanozymes Meet Single-Atom Catalysis, *Angew. Chem., Int. Ed.*, 2020, **59**, 2565–2576.
17 X. Zhang, G. Li, G. Chen, D. Wu, X. Zhou and Y. Wu, Single-atom nanozymes: A rising star for biosensing and biomedicine, *Coord. Chem. Rev.*, 2020, **418**, 213376.
18 W. Wu, L. Huang, E. Wang and S. Dong, Atomic engineering of single-atom nanozymes for enzyme-like catalysis, *Chem. Sci.*, 2020, **11**, 9741–9756.
19 C. Zhao, C. Xiong, X. Liu, M. Qiao, Z. Li, T. Yuan, J. Wang, Y. Qu, X. Wang, F. Zhou, Q. Xu, S. Wang, M. Chen, W. Wang, Y. Li, T. Yao, Y. Wu and Y. Li, Unraveling the enzyme-like activity of heterogeneous single atom catalyst, *Chem. Commun.*, 2019, **55**, 2285–2288.
20 J. Pei, R. Zhao, X. Mu, J. Wang, C. Liu and X. D. Zhang, Single-atom nanozymes for biological applications, *Biomater. Sci.*, 2020, **8**, 6428–6441.
21 R. Zhang, K. Fan and X. Yan, Nanozymes: created by learning from nature, *Sci. China: Life Sci.*, 2020, **63**, 1183–1200.
22 V. Kandathil and S. A. Patil, Single-atom nanozymes and environmental catalysis: A perspective, *Adv. Colloid Interface Sci.*, 2021, **294**, 102485.
23 L. Su, S. Qin, Z. Xie, L. Wang, K. Khan, A. K. Tareen, D. Li and H. Zhang, Multi-enzyme activity nanozymes for biosensing and disease treatment, *Coord. Chem. Rev.*, 2022, **473**, 214784.
24 D. Xu, L. Wu, H. Yao and L. Zhao, Catalase-Like Nanozymes: Classification, Catalytic Mechanisms, and Their Applications, *Small*, 2022, **18**, e2203400.

 

25 W. Yang, X. Yang, L. Zhu, H. Chu, X. Li and W. Xu, Nanozymes: Activity origin, catalytic mechanism, and biological application, *Coord. Chem. Rev.*, 2021, **448**, 214170.

26 F. Cao, L. Zhang, Y. You, L. Zheng, J. Ren and X. Qu, An Enzyme-Mimicking Single-Atom Catalyst as an Efficient Multiple Reactive Oxygen and Nitrogen Species Scavenger for Sepsis Management, *Angew. Chem., Int. Ed.*, 2020, **59**, 5108–5115.

27 Y. Chen, H. Zou, B. Yan, X. Wu, W. Cao, Y. Qian, L. Zheng and G. Yang, Atomically Dispersed Cu Nanozyme with Intensive Ascorbate Peroxidase Mimic Activity Capable of Alleviating ROS-Mediated Oxidation Damage, *Adv. Sci.*, 2022, **9**, e2103977.

28 Y. Chong, Q. Liu and C. Ge, Advances in oxidase-mimicking nanozymes: Classification, activity regulation and biomedical applications, *Nano Today*, 2021, **37**, 101076.

29 C. Jiang, T. He, Q. Tang, J. He, Q. Ren, D.-Y. Zhang, B. Gurram, N. T. Blum, Y. Chen, P. Huang and J. Lin, Nanozyme catalyzed cascade reaction for enhanced chemodynamic therapy of low-$H_2O_2$ tumor, *Appl. Mater. Today*, 2022, **26**, 101357.

30 D. Li, D. Dai, G. Xiong, S. Lan and C. Zhang, Metal-Based Nanozymes with Multienzyme-Like Activities as Therapeutic Candidates: Applications, Mechanisms, and Optimization Strategy, *Small*, 2022, e2205870, DOI: **10.1002/smll.202205870**.

31 P. Zhu, X. Xiong and D. Wang, Regulations of active moiety in single atom catalysts for electrochemical hydrogen evolution reaction, *Nano Res.*, 2022, **15**, 5792–5815.

32 M. Zandieh and J. Liu, Nanozyme Catalytic Turnover and Self-Limited Reactions, *ACS Nano*, 2021, **15**, 15645–15655.

33 R. Li and D. Wang, Understanding the structure-performance relationship of active sites at atomic scale, *Nano Res.*, 2022, **15**, 6888–6923.

34 Y. Huang, J. Ren and X. Qu, Nanozymes: Classification, Catalytic Mechanisms, Activity Regulation, and Applications, *Chem. Rev.*, 2019, **119**, 4357–4412.

35 X. Hai, S. Xi, S. Mitchell, K. Harrath, H. Xu, D. F. Akl, D. Kong, J. Li, Z. Li, T. Sun, H. Yang, Y. Cui, C. Su, X. Zhao, J. Li, J. Perez-Ramirez and J. Lu, Scalable two-step annealing method for preparing ultra-high-density single-atom catalyst libraries, *Nat. Nanotechnol.*, 2022, **17**, 174–181.

36 F. Meng, P. Zhu, L. Yang, L. Xia and H. Liu, Nanozymes with atomically dispersed metal centers: Structure–activity relationships and biomedical applications, *Chem. Eng. J.*, 2023, **452**, 139411.

37 Q. Shi, T. Yu, R. Wu and J. Liu, Metal-Support Interactions of Single-Atom Catalysts for Biomedical Applications, *ACS Appl. Mater. Interfaces*, 2021, **13**, 60815–60836.

38 N. Cheng and X. Sun, Single atom catalyst by atomic layer deposition technique, *Chin. J. Catal.*, 2017, **38**, 1508–1514.

39 H. Yan, Y. Lin, H. Wu, W. Zhang, Z. Sun, H. Cheng, W. Liu, C. Wang, J. Li, X. Huang, T. Yao, J. Yang, S. Wei and J. Lu, Bottom-up precise synthesis of stable platinum dimers on graphene, *Nat. Commun.*, 2017, **8**, 1070.

40 C. H. Choi, M. Kim, H. C. Kwon, S. J. Cho, S. Yun, H. T. Kim, K. J. Mayrhofer, H. Kim and M. Choi, Tuning selectivity of electrochemical reactions by atomically dispersed platinum catalyst, *Nat. Commun.*, 2016, **7**, 10922.

41 T. Gan, Q. He, H. Zhang, H. Xiao, Y. Liu, Y. Zhang, X. He and H. Ji, Unveiling the kilogram-scale gold single-atom catalysts via ball milling for preferential oxidation of CO in excess hydrogen, *Chem. Eng. J.*, 2020, **389**, 124490.

42 Y. Wu, L. Jiao, X. Luo, W. Xu, X. Wei, H. Wang, H. Yan, W. Gu, B. Z. Xu, D. Du, Y. Lin and C. Zhu, Oxidase-Like Fe-N-C Single-Atom Nanozymes for the Detection of Acetylcholinesterase Activity, *Small*, 2019, **15**, 1903108.

43 Y. Zou, S. A. Kazemi, G. Shi, J. Liu, Y. Yang, N. M. Bedford, K. Fan, Y. Xu, H. Fu, M. Dong, M. Al-Mamun, Y. L. Zhong, H. Yin, Y. Wang, P. Liu and H. Zhao, Ruthenium single–atom modulated Ti3C2Tx MXene for efficient alkaline electrocatalytic hydrogen production, *EcoMat*, 2022, **5**, e12274.

44 M. A. Denchy, L. Wang, B. R. Bilik, L. Hansen, S. Albornoz, F. Lizano, N. Blando, Z. Hicks, G. Gantefoer and K. H. Bowen, Ultrasmall Cluster Model for Investigating Single Atom Catalysis: Dehydrogenation of 1-Propanamine by Size-Selected Pt(1)Zr(2)O(7) Clusters Supported on HOPG, *J. Phys. Chem. A*, 2022, **126**, 7578–7590.

45 W. E. Kaden, T. Wu, W. A. Kunkel and S. L. Anderson, Electronic structure controls reactivity of size-selected Pd clusters adsorbed on TiO2 surfaces, *Science*, 2009, **326**, 826–829.

46 W. Fu, J. Wan, H. Zhang, J. Li, W. Chen, Y. Li, Z. Guo and Y. Wang, Photoinduced loading of electron-rich Cu single atoms by moderate coordination for hydrogen evolution, *Nat. Commun.*, 2022, **13**, 5496.

47 H. Wei, K. Huang, D. Wang, R. Zhang, B. Ge, J. Ma, B. Wen, S. Zhang, Q. Li, M. Lei, C. Zhang, J. Irawan, L. M. Liu and H. Wu, Iced photochemical reduction to synthesize atomically dispersed metals by suppressing nanocrystal growth, *Nat. Commun.*, 2017, **8**, 1490.

48 S. Ding, H.-A. Chen, O. Mekasuwandumrong, M. J. Hülsey, X. Fu, Q. He, J. Panpranot, C.-M. Yang and N. Yan, High-temperature flame spray pyrolysis induced stabilization of Pt single-atom catalysts, *Appl. Catal., B*, 2021, **281**, 119471.

49 A. A. Vernekar, D. Sinha, S. Srivastava, P. U. Paramasivam, P. D'Silva and G. Mugesh, An antioxidant nanozyme that uncovers the cytoprotective potential of vanadia nanowires, *Nat. Commun.*, 2014, **5**, 5301.

50 Y. Suda, N. Hosoya and K. Miki, Si submonolayer and monolayer digital growth operation techniques using Si2H6 as atomically controlled growth nanotechnology, *Appl. Surf. Sci.*, 2003, **216**, 424–430.

51 G. Vile, D. Albani, M. Nachtegaal, Z. Chen, D. Dontsova, M. Antonietti, N. Lopez and J. Perez-Ramirez, A stable single-site palladium catalyst for hydrogenations, *Angew. Chem., Int. Ed.*, 2015, **54**, 11265–11269.

52 Y. Fan, S. Liu, Y. Yi, H. Rong and J. Zhang, Catalytic Nanomaterials toward Atomic Levels for Biomedical

Applications: From Metal Clusters to Single-Atom Catalysts, *ACS Nano*, 2021, **15**, 2005–2037.
53 H. Song, M. Zhang and W. Tong, Single-Atom Nanozymes: Fabrication, Characterization, Surface Modification and Applications of ROS Scavenging and Antibacterial, *Molecules*, 2022, **27**, 5426.
54 A. Han, B. Wang, A. Kumar, Y. Qin, J. Jin, X. Wang, C. Yang, B. Dong, Y. Jia, J. Liu and X. Sun, Recent Advances for MOF–Derived Carbon–Supported Single–Atom Catalysts, *Small Methods*, 2019, **3**, 1800471.
55 B. Xu, S. Li, L. Zheng, Y. Liu, A. Han, J. Zhang, Z. Huang, H. Xie, K. Fan, L. Gao and H. Liu, A Bioinspired Five-Coordinated Single-Atom Iron Nanozyme for Tumor Catalytic Therapy, *Adv. Mater.*, 2022, **34**, e2107088.
56 S. Chen, W. Lu, R. Xu, J. Tan and X. Liu, Pyrolysis-free and universal synthesis of metal-NC single-atom nanozymes with dual catalytic sites for cytoprotection, *Carbon*, 2023, **201**, 439–448.
57 Q. Wang, D. Zhang, Y. Chen, W.-F. Fu and X.-J. Lv, Single-Atom Catalysts for Photocatalytic Reactions, *ACS Sustainable Chem. Eng.*, 2019, **7**, 6430–6443.
58 H. Xiang, W. Feng and Y. Chen, Single-Atom Catalysts in Catalytic Biomedicine, *Adv. Mater.*, 2020, **32**, 1905994.
59 J. Wu, L. Xiong, B. Zhao, M. Liu and L. Huang, Densely Populated Single Atom Catalysts, *Small Methods*, 2019, **4**, 1900540.
60 Y. Chen, Q. Yuchi, T. Li, G. Yang, J. Miao, C. Huang, J. Liu, A. Li, Y. Qin and L. Zhang, Precise engineering of ultra-thin Fe2O3 decorated Pt-based nanozymes via atomic layer deposition to switch off undesired activity for enhanced sensing performance, *Sens. Actuators, B*, 2020, **305**, 127436.
61 F. Qin, J. Zhang, Z. Zhou, H. Xu, L. Cui, Z. Lv and Y. Qin, TiO2 Nanoflowers Decorated with FeOx Nanocluster and Single Atoms by Atomic Layer Deposition for Peroxidase-Mimicking Nanozymes, *ACS Appl. Nano Mater.*, 2022, **5**, 13090–13099.
62 J. H. Kim, D. Shin, J. Lee, D. S. Baek, T. J. Shin, Y. T. Kim, H. Y. Jeong, J. H. Kwak, H. Kim and S. H. Joo, A General Strategy to Atomically Dispersed Precious Metal Catalysts for Unravelling Their Catalytic Trends for Oxygen Reduction Reaction, *ACS Nano*, 2020, **14**, 1990–2001.
63 Q. Zhou, J. Cai, Z. Zhang, R. Gao, B. Chen, G. Wen, L. Zhao, Y. Deng, H. Dou, X. Gong, Y. Zhang, Y. Hu, A. Yu, X. Sui, Z. Wang and Z. Chen, A Gas-Phase Migration Strategy to Synthesize Atomically Dispersed Mn-N-C Catalysts for Zn-Air Batteries, *Small Methods*, 2021, **5**, 2100024.
64 L. Shen, D. Ye, H. Zhao and J. Zhang, Perspectives for Single-Atom Nanozymes: Advanced Synthesis, Functional Mechanisms, and Biomedical Applications, *Anal. Chem.*, 2021, **93**, 1221–1231.
65 T. Gao, Z. Zhu, Y. Li, H. Hu, H. Rong, W. Liu, T. Yang and X. Zhang, Highly efficient electromagnetic absorption on ZnN4-based MOFs-derived carbon composites, *Carbon*, 2021, **177**, 44–51.
66 X. Liu, F. He, Y. Lu, S. Wang, C. Zhao, S. Wang, X. Duan, H. Zhang, X. Zhao, H. Sun, J. Zhang and S. Wang, The double-edged effect of single atom metals on photocatalysis, *Chem. Eng. J.*, 2023, **453**, 139833.
67 E. Luo, H. Zhang, X. Wang, L. Gao, L. Gong, T. Zhao, Z. Jin, J. Ge, Z. Jiang, C. Liu and W. Xing, Single-Atom Cr-N(4) Sites Designed for Durable Oxygen Reduction Catalysis in Acid Media, *Angew. Chem., Int. Ed.*, 2019, **58**, 12469–12475.
68 L. Yan, L. Xie, X. L. Wu, M. Qian, J. Chen, Y. Zhong and Y. Hu, Precise regulation of pyrrole–type single–atom Mn–N4 sites for superior pH–universal oxygen reduction, *Carbon Energy*, 2021, **3**, 856–865.
69 M. Zhang, C. Lai, B. Li, S. Liu, D. Huang, F. Xu, X. Liu, L. Qin, Y. Fu, L. Li, H. Yi and L. Chen, MXenes as Superexcellent Support for Confining Single Atom: Properties, Synthesis, and Electrocatalytic Applications, *Small*, 2021, **17**, e2007113.
70 N. Cheng, J. C. Li, D. Liu, Y. Lin and D. Du, Single-Atom Nanozyme Based on Nanoengineered Fe-N-C Catalyst with Superior Peroxidase-Like Activity for Ultrasensitive Bioassays, *Small*, 2019, **15**, e1901485.
71 M. S. Kim, J. Lee, H. S. Kim, A. Cho, K. H. Shim, T. N. Le, S. S. A. An, J. W. Han, M. I. Kim and J. Lee, Heme Cofactor–Resembling Fe–N Single Site Embedded Graphene as Nanozymes to Selectively Detect $H_2O_2$ with High Sensitivity, *Adv. Funct. Mater.*, 2019, **30**, 1905410.
72 G. Balraj, R. Gurrapu, A. Anil Kumar, V. Sumalatha and D. Ayodhya, Facile synthesis and characterization of noble metals decorated g-C3N4 (g-C3N4/Pt and g-C3N4/Pd) nanocomposites for efficient photocatalytic production of Schiff bases, *Results Chem.*, 2022, **4**, 100597.
73 F. K. Kessler, Y. Zheng, D. Schwarz, C. Merschjann, W. Schnick, X. Wang and M. J. Bojdys, Functional carbon nitride materials—design strategies for electrochemical devices, *Nat. Rev. Mater.*, 2017, **2**, 17030.
74 S.-F. Duan, C.-L. Tao, Y.-Y. Geng, X.-Q. Yao, X.-W. Kang, J.-Z. Su, I. Rodríguez-Gutiérrez, M. Kan, M. Romero, Y. Sun, Y.-X. Zhao, D.-D. Qin and Y. Yan, Phosphorus-doped Isotype g-C3N4/g-C3N4: An Efficient Charge Transfer System for Photoelectrochemical Water Oxidation, *ChemCatChem*, 2019, **11**, 729–736.
75 Y. Meng, L. Zhang, H. Jiu, Q. Zhang, H. Zhang, W. Ren, Y. Sun and D. Li, Construction of g-C3N4/ZIF-67 photocatalyst with enhanced photocatalytic CO2 reduction activity, *Mater. Sci. Semicond. Process.*, 2019, **95**, 35–41.
76 T. S. Safaei, A. Mepham, X. Zheng, Y. Pang, C. T. Dinh, M. Liu, D. Sinton, S. O. Kelley and E. H. Sargent, High-Density Nanosharp Microstructures Enable Efficient CO(2) Electroreduction, *Nano Lett.*, 2016, **16**, 7224–7228.
77 Y. Fan, W. Zhang, Y. Liu, Z. Zeng, X. Quan and H. Zhao, Three-Dimensional Branched Crystal Carbon Nitride with Enhanced Intrinsic Peroxidase-Like Activity: A Hypersensitive Platform for Colorimetric Detection, *ACS Appl. Mater. Interfaces*, 2019, **11**, 17467–17474.
78 J. Jiang, Z. Xiong, H. Wang, G. Liao, S. Bai, J. Zou, P. Wu, P. Zhang and X. Li, Sulfur-doped g-C3N4/g-C3N4 isotype

 

step-scheme heterojunction for photocatalytic H2 evolution, *J. Mater. Sci. Technol.*, 2022, **118**, 15–24.
79 Z. Wang, K. Dong, Z. Liu, Y. Zhang, Z. Chen, H. Sun, J. Ren and X. Qu, Activation of biologically relevant levels of reactive oxygen species by Au/g-C(3)N(4) hybrid nanozyme for bacteria killing and wound disinfection, *Biomaterials*, 2017, **113**, 145–157.
80 Y. Li, Z. He, L. Liu, Y. Jiang, W.-J. Ong, Y. Duan, W. Ho and F. Dong, Inside-and-out modification of graphitic carbon nitride (g-C3N4) photocatalysts via defect engineering for energy and environmental science, *Nano Energy*, 2023, **105**, 108032.
81 J. Xing, N. Wang, X. Li, J. Wang, M. Taiwaikuli, X. Huang, T. Wang, L. Zhou and H. Hao, Synthesis and modifications of g-C3N4-based materials and their applications in wastewater pollutants removal, *J. Environ. Chem. Eng.*, 2022, **10**, 108782.
82 Y. Yang, F. Yang, Z. Li, N. Zhang and S. Hao, Z-scheme g-C3N4/C/S-g-C3N4 heterostructural nanotube with enhanced porous structure and visible light driven photocatalysis, *Microporous Mesoporous Mater.*, 2021, **314**, 110891.
83 D. Wang and Y. Zhao, Single-atom engineering of metal-organic frameworks toward healthcare, *Chem*, 2021, **7**, 2635–2671.
84 B. Xu, Z. Huang, Y. Liu, S. Li and H. Liu, MOF-based nanomedicines inspired by structures of natural active components, *Nano Today*, 2023, **48**, 101690.
85 S. Nazri, M. Khajeh, A. R. Oveisi, R. Luque, E. Rodríguez-Castellón and M. Ghaffari-Moghaddam, Thiol-functionalized PCN-222 MOF for fast and selective extraction of gold ions from aqueous media, *Sep. Purif. Technol.*, 2021, **259**, 118197.
86 Z. Zhou, J. Zhang, S. Mukherjee, S. Hou, R. Khare, M. Döblinger, O. Tomanec, M. Otyepka, M. Koch, P. Gao, L. Zhou, W. Li and R. A. Fischer, Porphyrinic MOF derived Single-atom electrocatalyst enables methanol oxidation, *Chem. Eng. J.*, 2022, **449**, 137888.
87 Z. Wang, Q. Sun, B. Liu, Y. Kuang, A. Gulzar, F. He, S. Gai, P. Yang and J. Lin, Recent advances in porphyrin-based MOFs for cancer therapy and diagnosis therapy, *Coord. Chem. Rev.*, 2021, **439**, 213945.
88 W. Y. Gao, M. Chrzanowski and S. Ma, Metal-metalloporphyrin frameworks: a resurging class of functional materials, *Chem. Soc. Rev.*, 2014, **43**, 5841–5866.
89 G. Zhan, Q. Xu, Z. Zhang, Z. Wei, T. Yong, N. Bie, X. Zhang, X. Li, J. Li, L. Gan and X. Yang, Biomimetic sonodynamic therapy-nanovaccine integration platform potentiates Anti-PD-1 therapy in hypoxic tumors, *Nano Today*, 2021, **38**, 101195.
90 S. Daliran, A. R. Oveisi, Y. Peng, A. Lopez-Magano, M. Khajeh, R. Mas-Balleste, J. Aleman, R. Luque and H. Garcia, Correction: Metal-organic framework (MOF)-, covalent-organic framework (COF)-, and porous-organic polymers (POP)-catalyzed selective C-H bond activation and functionalization reactions, *Chem. Soc. Rev.*, 2022, **51**, 8140.
91 Z. Li, S. Qiu, Y. Song, S. Huang, J. Gao, L. Sun and J. Hou, Engineering single-atom active sites anchored covalent organic frameworks for efficient metallaphotoredox CN cross-coupling reactions, *Sci. Bull.*, 2022, **67**, 1971–1981.
92 P. Dong, Y. Wang, A. Zhang, T. Cheng, X. Xi and J. Zhang, Platinum Single Atoms Anchored on a Covalent Organic Framework: Boosting Active Sites for Photocatalytic Hydrogen Evolution, *ACS Catal.*, 2021, **11**, 13266–13279.
93 K. Chi, Y. Wu, X. Wang, Q. Zhang, W. Gao, L. Yang, X. Chen, D. Chang, Y. Zhang, T. Shen, X. Lu, Y. Zhao and Y. Liu, Single Atom Catalysts with Out-of-Plane Coordination Structure on Conjugated Covalent Organic Frameworks, *Small*, 2022, **18**, e2203966.
94 Z. Dong, L. Zhang, J. Gong and Q. Zhao, Covalent organic framework nanorods bearing single Cu sites for efficient photocatalysis, *Chem. Eng. J.*, 2021, **403**, 126383.
95 M. Kou, W. Liu, Y. Wang, J. Huang, Y. Chen, Y. Zhou, Y. Chen, M. Ma, K. Lei, H. Xie, P. K. Wong and L. Ye, Photocatalytic CO2 conversion over single-atom MoN2 sites of covalent organic framework, *Appl. Catal., B*, 2021, **291**, 120146.
96 Q. Tang, S. Cao, T. Ma, X. Xiang, H. Luo, P. Borovskikh, R. D. Rodriguez, Q. Guo, L. Qiu and C. Cheng, Engineering Biofunctional Enzyme–Mimics for Catalytic Therapeutics and Diagnostics, *Adv. Funct. Mater.*, 2020, **31**, 2007475.
97 M. Abbas and M. A. Z. G. Sial, New Horizon in stabilization of single atoms on metal-oxide supports for $CO_2$ reduction, *Nano Mater. Sci.*, 2021, **3**, 368–389.
98 B. Han, Y. Guo, Y. Huang, W. Xi, J. Xu, J. Luo, H. Qi, Y. Ren, X. Liu, B. Qiao and T. Zhang, Strong Metal-Support Interactions between Pt Single Atoms and TiO(2), *Angew. Chem., Int. Ed.*, 2020, **59**, 11824–11829.
99 Z. Liu, L. Sun, Q. Zhang, Z. Teng, H. Sun and C. Su, TiO2-supported Single-atom Catalysts: Synthesis, Structure, and Application, *Chem. Res. Chin. Univ.*, 2022, **38**, 1123–1138.
100 Y.-Q. Su, Y. Wang, J.-X. Liu, I. A. W. Filot, K. Alexopoulos, L. Zhang, V. Muravev, B. Zijlstra, D. G. Vlachos and E. J. M. Hensen, Theoretical Approach To Predict the Stability of Supported Single-Atom Catalysts, *ACS Catal.*, 2019, **9**, 3289–3297.
101 X. Liao, Y. Zhao, C. Liu, X. Li, Y. Sun, K. Kato, M. Yamauchi and Z. Jiang, Low temperature surface oxygen activation in crystalline $MnO_2$ triggered by lattice confined Pd single atoms, *J. Energy Chem.*, 2021, **62**, 136–144.
102 Y. Wang, K. Qi, S. Yu, G. Jia, Z. Cheng, L. Zheng, Q. Wu, Q. Bao, Q. Wang, J. Zhao, X. Cui and W. Zheng, Revealing the Intrinsic Peroxidase-Like Catalytic Mechanism of Heterogeneous Single-Atom Co-MoS(2), *Nano-Micro Lett.*, 2019, **11**, 102.
103 B. Chang, L. Zhang, S. Wu, Z. Sun and Z. Cheng, Engineering single-atom catalysts toward biomedical applications, *Chem. Soc. Rev.*, 2022, **51**, 3688–3734.
104 X. Wei, S. Song, W. Song, W. Xu, L. Jiao, X. Luo, N. Wu, H. Yan, X. Wang, W. Gu, L. Zheng and C. Zhu, Fe(3)

C-Assisted Single Atomic Fe Sites for Sensitive Electrochemical Biosensing, *Anal. Chem.*, 2021, **93**, 5334–5342.

105 F. Wu, C. Pan, C. T. He, Y. Han, W. Ma, H. Wei, W. Ji, W. Chen, J. Mao, P. Yu, D. Wang, L. Mao and Y. Li, Single-Atom Co-N(4) Electrocatalyst Enabling Four-Electron Oxygen Reduction with Enhanced Hydrogen Peroxide Tolerance for Selective Sensing, *J. Am. Chem. Soc.*, 2020, **142**, 16861–16867.

106 B. Jiang and M. Liang, Advances in Single–Atom Nanozymes Research, *Chin. J. Chem.*, 2020, **39**, 174–180.

107 S. Fu, C. Zhu, D. Su, J. Song, S. Yao, S. Feng, M. H. Engelhard, D. Du and Y. Lin, Porous Carbon-Hosted Atomically Dispersed Iron-Nitrogen Moiety as Enhanced Electrocatalysts for Oxygen Reduction Reaction in a Wide Range of pH, *Small*, 2018, **14**, e1703118.

108 X. Niu, Q. Shi, W. Zhu, D. Liu, H. Tian, S. Fu, N. Cheng, S. Li, J. N. Smith, D. Du and Y. Lin, Unprecedented peroxidase-mimicking activity of single-atom nanozyme with atomically dispersed Fe-N(x) moieties hosted by MOF derived porous carbon, *Biosens. Bioelectron.*, 2019, **142**, 111495.

109 W. Liu, L. Chu, C. Zhang, P. Ni, Y. Jiang, B. Wang, Y. Lu and C. Chen, Hemin-assisted synthesis of peroxidase-like Fe-N-C nanozymes for detection of ascorbic acid-generating bio-enzymes, *Chem. Eng. J.*, 2021, **415**, 128876.

110 Y. Feng, J. Qin, Y. Zhou, Q. Yue and J. Wei, Spherical mesoporous Fe-N-C single-atom nanozyme for photothermal and catalytic synergistic antibacterial therapy, *J. Colloid Interface Sci.*, 2022, **606**, 826–836.

111 X. Wu, Y. Sun, T. He, Y. Zhang, G. J. Zhang, Q. Liu and S. Chen, Iron, Nitrogen-Doped Carbon Aerogels for Fluorescent and Electrochemical Dual-Mode Detection of Glucose, *Langmuir*, 2021, **37**, 11309–11315.

112 L. Huang, J. Chen, L. Gan, J. Wang and S. Dong, Single-atom nanozymes, *Sci. Adv.*, 2019, **5**, 46.

113 Q. Chen, X. Zhang, S. Li, J. Tan, C. Xu and Y. Huang, MOF-derived Co3O4@Co-Fe oxide double-shelled nanocages as multi-functional specific peroxidase-like nanozyme catalysts for chemo/biosensing and dye degradation, *Chem. Eng. J.*, 2020, **395**, 125130.

114 B. Liu, Y. Xue, Z. Gao, K. Tang, G. Wang, Z. Chen and X. Zuo, Antioxidant identification using a colorimetric sensor array based on Co-N-C nanozyme, *Colloids Surf., B*, 2021, **208**, 112060.

115 L. Sun, Y. Yan, S. Chen, Z. Zhou, W. Tao, C. Li, Y. Feng and F. Wang, Co-N-C single-atom nanozymes with oxidase-like activity for highly sensitive detection of biothiols, *Anal. Bioanal. Chem.*, 2022, **414**, 1857–1865.

116 S. Cai, J. Liu, J. Ding, Z. Fu, H. Li, Y. Xiong, Z. Lian, R. Yang and C. Chen, Tumor-Microenvironment-Responsive Cascade Reactions by a Cobalt-Single-Atom Nanozyme for Synergistic Nanocatalytic Chemotherapy, *Angew. Chem., Int. Ed.*, 2022, **61**, e202204502.

117 Y. Song, T. He, Y. Zhang, C. Yin, Y. Chen, Q. Liu, Y. Zhang and S. Chen, Cobalt single atom sites in carbon aerogels for ultrasensitive enzyme-free electrochemical detection of glucose, *J. Electroanal. Chem.*, 2022, **906**, 116024.

118 B. Xu, H. Wang, W. Wang, L. Gao, S. Li, X. Pan, H. Wang, H. Yang, X. Meng, Q. Wu, L. Zheng, S. Chen, X. Shi, K. Fan, X. Yan and H. Liu, A Single-Atom Nanozyme for Wound Disinfection Applications, *Angew. Chem., Int. Ed.*, 2019, **58**, 4911–4916.

119 Z. Li, B. Li and C. Yu, Atomic Aerogel Materials (or single atom aerogels): an Interesting New Paradigm in Materials Science and Catalysis Science, *Adv. Mater.*, 2023, e2211221, DOI: **10.1002/adma.202211221**.

120 C. B. Ma, Y. Xu, L. Wu, Q. Wang, J. J. Zheng, G. Ren, X. Wang, X. Gao, M. Zhou, M. Wang and H. Wei, Guided Synthesis of a Mo/Zn Dual Single-Atom Nanozyme with Synergistic Effect and Peroxidase-like Activity, *Angew. Chem., Int. Ed.*, 2022, **61**, e202116170.

121 Y. Kong, Y. Li, X. Sang, B. Yang, Z. Li, S. Zheng, Q. Zhang, S. Yao, X. Yang, L. Lei, S. Zhou, G. Wu and Y. Hou, Atomically Dispersed Zinc(I) Active Sites to Accelerate Nitrogen Reduction Kinetics for Ammonia Electrosynthesis, *Adv. Mater.*, 2022, **34**, e2103548.

122 K. S. Siddiqi, A. Ur Rahman, Tajuddin and A. Husen, Properties of Zinc Oxide Nanoparticles and Their Activity Against Microbes, *Nanoscale Res. Lett.*, 2018, **13**, 141.

123 B. Qiao, A. Wang, X. Yang, L. F. Allard, Z. Jiang, Y. Cui, J. Liu, J. Li and T. Zhang, Single-atom catalysis of CO oxidation using Pt1/FeOx, *Nat. Chem.*, 2011, **3**, 634–641.

124 Y. Xin, N. Zhang, Y. Lv, J. Wang, Q. Li and Z. Zhang, From nanoparticles to single atoms for Pt/$CeO_2$: Synthetic strategies, characterizations and applications, *J. Rare Earths*, 2020, **38**, 850–862.

125 X. Ye, H. Wang, Y. Lin, X. Liu, L. Cao, J. Gu and J. Lu, Insight of the stability and activity of platinum single atoms on ceria, *Nano Res.*, 2019, **12**, 1401–1409.

126 R. Yan, S. Sun, J. Yang, W. Long, J. Wang, X. Mu, Q. Li, W. Hao, S. Zhang, H. Liu, Y. Gao, L. Ouyang, J. Chen, S. Liu, X. D. Zhang and D. Ming, Nanozyme-Based Bandage with Single-Atom Catalysis for Brain Trauma, *ACS Nano*, 2019, **13**, 11552–11560.

127 Y. Chen, P. Wang, H. Hao, J. Hong, H. Li, S. Ji, A. Li, R. Gao, J. Dong, X. Han, M. Liang, D. Wang and Y. Li, Thermal Atomization of Platinum Nanoparticles into Single Atoms: An Effective Strategy for Engineering High-Performance Nanozymes, *J. Am. Chem. Soc.*, 2021, **143**, 18643–18651.

128 Y. Fan, X. Gan, H. Zhao, Z. Zeng, W. You and X. Quan, Multiple application of SAzyme based on carbon nitride nanorod-supported Pt single-atom for $H_2O_2$ detection, antibiotic detection and antibacterial therapy, *Chem. Eng. J.*, 2022, **427**, 131572.

129 S. H. Chang, B. Y. Chen and J. X. Lin, Toxicity assessment and selective leaching characteristics of Cu-Al-Ni shape memory alloys in biomaterials applications, *J. Appl. Biomater. Funct. Mater.*, 2016, **14**, e59–e64.

130 J. Zhu, Q. Li, X. Li, X. Wu, T. Yuan and Y. Yang, Simulated Enzyme Activity and Efficient Antibacterial Activity of

 

Copper-Doped Single-Atom Nanozymes, *Langmuir*, 2022, **38**, 6860–6870.

131 G. Song, J. C. Li, Z. Majid, W. Xu, X. He, Z. Yao, Y. Luo, K. Huang and N. Cheng, Phosphatase-like activity of single-atom CeNC nanozyme for rapid detection of Al(3), *Food Chem.*, 2022, **390**, 133127.

132 C. Mochizuki, Y. Inomata, S. Yasumura, M. Lin, A. Taketoshi, T. Honma, N. Sakaguchi, M. Haruta, K.-I. Shimizu, T. Ishida and T. Murayama, Defective NiO as a Stabilizer for Au Single-Atom Catalysts, *ACS Catal.*, 2022, 6149–6158, DOI: **10.1021/acscatal.2c00108**.

133 C. Rong, X. Shen, Y. Wang, L. Thomsen, T. Zhao, Y. Li, X. Lu, R. Amal and C. Zhao, Electronic Structure Engineering of Single–Atom Ru Sites via Co–N4 Sites for Bifunctional pH–Universal Water Splitting, *Adv. Mater.*, 2022, **34**, 2110103.

134 R. Tian, H. Ma, W. Ye, Y. Li, S. Wang, Z. Zhang, S. Liu, M. Zang, J. Hou, J. Xu, Q. Luo, H. Sun, F. Bai, Y. Yang and J. Liu, Se–Containing MOF Coated Dual–Fe–Atom Nanozymes With Multi–Enzyme Cascade Activities Protect Against Cerebral Ischemic Reperfusion Injury, *Adv. Funct. Mater.*, 2022, **32**, 2204025.

135 M. Fan, J. Cui, J. Wu, R. Vajtai, D. Sun and P. M. Ajayan, Improving the Catalytic Activity of Carbon-Supported Single Atom Catalysts by Polynary Metal or Heteroatom Doping, *Small*, 2020, **16**, e1906782.

136 S. Ji, B. Jiang, H. Hao, Y. Chen, J. Dong, Y. Mao, Z. Zhang, R. Gao, W. Chen, R. Zhang, Q. Liang, H. Li, S. Liu, Y. Wang, Q. Zhang, L. Gu, D. Duan, M. Liang, D. Wang, X. Yan and Y. Li, Matching the kinetics of natural enzymes with a single-atom iron nanozyme, *Nat. Catal.*, 2021, **4**, 407–417.

137 R. Li, X. He, R. Javed, J. Cai, H. Cao, X. Liu, Q. Chen, D. Ye and H. Zhao, Switching on-off-on colorimetric sensor based on Fe-N/S-C single-atom nanozyme for ultrasensitive and multimodal detection of Hg(2), *Sci. Total Environ.*, 2022, **834**, 155428.

138 C.-C. Hou, H.-F. Wang, C. Li and Q. Xu, From metal–organic frameworks to single/dual-atom and cluster metal catalysts for energy applications, *Energy Environ. Sci.*, 2020, **13**, 1658–1693.

139 Q. Chen, Y. Liu, Y. Lu, Y. Hou, X. Zhang, W. Shi and Y. Huang, Atomically dispersed Fe/Bi dual active sites single-atom nanozymes for cascade catalysis and peroxymonosulfate activation to degrade dyes, *J. Hazard. Mater.*, 2022, **422**, 126929.

140 G. Darabdhara, J. Bordoloi, P. Manna and M. R. Das, Biocompatible bimetallic Au-Ni doped graphitic carbon nitride sheets: A novel peroxidase-mimicking artificial enzyme for rapid and highly sensitive colorimetric detection of glucose, *Sens. Actuators, B*, 2019, **285**, 277–290.

141 H. Zhang and N. Toshima, Fabrication of catalytically active AgAu bimetallic nanoparticles by physical mixture of small Au clusters with Ag ions, *Appl. Catal., A*, 2012, **447–448**, 81–88.

142 Y. Wang, Z. Zhang, G. Jia, L. Zheng, J. Zhao and X. Cui, Elucidating the mechanism of the structure-dependent enzymatic activity of Fe-N/C oxidase mimics, *Chem. Commun.*, 2019, **55**, 5271–5274.

143 J. Chen, L. Huang, Q. Wang, W. Wu, H. Zhang, Y. Fang and S. Dong, Bio-inspired nanozyme: a hydratase mimic in a zeolitic imidazolate framework, *Nanoscale*, 2019, **11**, 5960–5966.

144 H. Liang, F. Lin, Z. Zhang, B. Liu, S. Jiang, Q. Yuan and J. Liu, Multicopper Laccase Mimicking Nanozymes with Nucleotides as Ligands, *ACS Appl. Mater. Interfaces*, 2017, **9**, 1352–1360.

145 J. Li, W. Liu, X. Wu and X. Gao, Mechanism of pH-switchable peroxidase and catalase-like activities of gold, silver, platinum and palladium, *Biomaterials*, 2015, **48**, 37–44.

146 P. Yin, T. Yao, Y. Wu, L. Zheng, Y. Lin, W. Liu, H. Ju, J. Zhu, X. Hong, Z. Deng, G. Zhou, S. Wei and Y. Li, Single Cobalt Atoms with Precise N-Coordination as Superior Oxygen Reduction Reaction Catalysts, *Angew. Chem., Int. Ed.*, 2016, **55**, 10800–10805.

147 M. Lu, C. Wang, Y. Ding, M. Peng, W. Zhang, K. Li, W. Wei and Y. Lin, Fe-N/C single-atom catalysts exhibiting multienzyme activity and ROS scavenging ability in cells, *Chem. Commun.*, 2019, **55**, 14534–14537.

148 Y. Wang, R. Du, L. Y. S. Lee and K. Y. Wong, Rational design and structural engineering of heterogeneous single-atom nanozyme for biosensing, *Biosens. Bioelectron.*, 2022, **216**, 114662.

149 G. Song, Q. Zhang, S. Liang, Y. Yao, M. Feng, Z. Majid, X. He, K. Huang, J.-C. Li and N. Cheng, Oxidation activity modulation of a single atom Ce-N-C nanozyme enabling a time-resolved sensor to detect $Fe^{3+}$ and $Cr^{6+}$, *J. Mater. Chem. C*, 2022, **10**, 15656–15663.

150 X. Zhou, M. Wang, J. Chen, X. Xie and X. Su, Peroxidase-like activity of Fe-N-C single-atom nanozyme based colorimetric detection of galactose, *Anal. Chim. Acta*, 2020, **1128**, 72–79.

151 H. Yan, L. Jiao, H. Wang, Y. Zhu, Y. Chen, L. Shuai, M. Gu, M. Qiu, W. Gu and C. Zhu, Single-atom Bi-anchored Au hydrogels with specifically boosted peroxidase-like activity for cascade catalysis and sensing, *Sens. Actuators, B*, 2021, **343**, 130108.

152 S. Wang, Z. Hu, Q. Wei, H. Zhang, W. Tang, Y. Sun, H. Duan, Z. Dai, Q. Liu and X. Zheng, Diatomic active sites nanozymes: Enhanced peroxidase-like activity for dopamine and intracellular $H_2O_2$ detection, *Nano Res.*, 2022, **15**, 4266–4273.

153 M. Feng, Q. Zhang, X. Chen, D. Deng, X. Xie and X. Yang, Controllable synthesis of boron-doped Zn-N-C single-atom nanozymes for the ultrasensitive colorimetric detection of p-phenylenediamine, *Biosens. Bioelectron.*, 2022, **210**, 114294.

154 W. Wu, L. Huang, X. Zhu, J. Chen, D. Chao, M. Li, S. Wu and S. Dong, Reversible inhibition of the oxidase-like activity of Fe single-atom nanozymes for drug detection, *Chem. Sci.*, 2022, **13**, 4566–4572.

155 F. X. Hu, T. Hu, S. Chen, D. Wang, Q. Rao, Y. Liu, F. Dai, C. Guo, H. B. Yang and C. M. Li, Single-Atom Cobalt-Based Electrochemical Biomimetic Uric Acid Sensor with Wide Linear Range and Ultralow Detection Limit, *Nano-Micro Lett.*, 2020, **13**, 1–13.

156 Y. Liu, P. Zhao, Y. Liang, Y. Chen, J. Pu, J. Wu, Y. Yang, Y. Ma, Z. Huang, H. Luo, D. Huo and C. Hou, Single-atom nanozymes Co-N-C as an electrochemical sensor for detection of bioactive molecules, *Talanta*, 2023, **254**, 124171.

157 Q. H. Nguyen, D. H. Lee, P. T. Nguyen, P. G. Le and M. I. Kim, Foldable paper microfluidic device based on single iron site-containing hydrogel nanozyme for efficient glucose biosensing, *Chem. Eng. J.*, 2023, **454**, 140541.

158 W. Wu, S. Xia, Y. Liu, C. Ma, Z. Lyu, M. Zhao, S. Ding and Q. Hu, Single-atom catalysts with peroxidase-like activity boost gel-sol transition-based biosensing, *Biosens. Bioelectron.*, 2023, **225**, 115112.

159 S. Li, D. Liu, B. Wu, H. Sun, X. Liu, H. Zhang, N. Ding and L. Wu, One-pot synthesis of a peroxidase-like nanozyme and its application in visual assay for tyrosinase activity, *Talanta*, 2022, **239**, 123088.

160 M. Wang, L. Liu, X. Xie, X. Zhou, Z. Lin and X. Su, Single-atom iron containing nanozyme with peroxidase-like activity and copper nanoclusters based ratio fluorescent strategy for acetylcholinesterase activity sensing, *Sens. Actuators, B*, 2020, **313**, 128023.

161 X. Niu, N. Cheng, X. Ruan, D. Du and Y. Lin, Review—Nanozyme-Based Immunosensors and Immunoassays: Recent Developments and Future Trends, *J. Electrochem. Soc.*, 2019, **167**, 037508.

162 L. Sun, C. Li, Y. Yan, Y. Yu, H. Zhao, Z. Zhou, F. Wang and Y. Feng, Engineering DNA/Fe-N-C single-atom nanozymes interface for colorimetric biosensing of cancer cells, *Anal. Chim. Acta*, 2021, **1180**, 338856.

163 B. Jiang, Z. Guo and M. Liang, Recent progress in single-atom nanozymes research, *Nano Res.*, 2022, 1–12, DOI: 10.1007/s12274-022-4856-7.

164 D. Wang, H. Wu, S. Z. F. Phua, G. Yang, W. Qi Lim, L. Gu, C. Qian, H. Wang, Z. Guo, H. Chen and Y. Zhao, Self-assembled single-atom nanozyme for enhanced photodynamic therapy treatment of tumor, *Nat. Commun.*, 2020, **11**, 357.

165 M. Chang, Z. Hou, M. Wang, C. Yang, R. Wang, F. Li, D. Liu, T. Peng, C. Li and J. Lin, Single-Atom Pd Nanozyme for Ferroptosis-Boosted Mild-Temperature Photothermal Therapy, *Angew. Chem., Int. Ed.*, 2021, **60**, 12971–12979.

166 Y. Zou, B. Jin, H. Li, X. Wu, Y. Liu, H. Zhao, D. Zhong, L. Wang, W. Chen, M. Wen and Y. N. Liu, Cold Nanozyme for Precise Enzymatic Antitumor Immunity, *ACS Nano*, 2022, **16**, 21491–21504.

167 Y. Zhu, W. Wang, P. Gong, Y. Zhao, Y. Pan, J. Zou, R. Ao, J. Wang, H. Cai, H. Huang, M. Yu, H. Wang, L. Lin, X. Chen and Y. Wu, Enhancing Catalytic Activity of a Nickel Single Atom Enzyme by Polynary Heteroatom Doping for Ferroptosis-Based Tumor Therapy, *ACS Nano*, 2023, 3064–3076, DOI: 10.1021/acsnano.2c11923.

168 B. Lin, H. Chen, D. Liang, W. Lin, X. Qi, H. Liu and X. Deng, Acidic pH and High-H(2)O(2) Dual Tumor Microenvironment-Responsive Nanocatalytic Graphene Oxide for Cancer Selective Therapy and Recognition, *ACS Appl. Mater. Interfaces*, 2019, **11**, 11157–11166.

169 H. He, Z. Fei, T. Guo, Y. Hou, D. Li, K. Wang, F. Ren, K. Fan, D. Zhou, C. Xie, C. Wang and X. Lu, Bioadhesive injectable hydrogel with phenolic carbon quantum dot supported Pd single atom nanozymes as a localized immunomodulation niche for cancer catalytic immunotherapy, *Biomaterials*, 2022, **280**, 121272.

170 N. Feng, Q. Li, Q. Bai, S. Xu, J. Shi, B. Liu and J. Guo, Development of an Au-anchored Fe Single-atom nanozyme for biocatalysis and enhanced tumor photothermal therapy, *J. Colloid Interface Sci.*, 2022, **618**, 68–77.

171 Y. Zhu, W. Wang, J. Cheng, Y. Qu, Y. Dai, M. Liu, J. Yu, C. Wang, H. Wang, S. Wang, C. Zhao, Y. Wu and Y. Liu, Stimuli-Responsive Manganese Single-Atom Nanozyme for Tumor Therapy via Integrated Cascade Reactions, *Angew. Chem., Int. Ed.*, 2021, **60**, 9480–9488.

172 Y. Xing, J. Xiu, M. Zhou, T. Xu, M. Zhang, H. Li, X. Li, X. Du, T. Ma and X. Zhang, Copper Single-Atom Jellyfish-like Nanomotors for Enhanced Tumor Penetration and Nanocatalytic Therapy, *ACS Nano*, 2023, **17**(7), 6789–6799.

173 T. Li, L. Chen, X. Fu, Z. Liu, S. Zhu, Y. Chen and J. Zhang, Iron Single-Atom nanocatalysts in response to tumor microenvironment for highly efficient Chemo-chemodynamic therapy, *J. Ind. Eng. Chem.*, 2022, **112**, 210–217.

174 Q. Chen, M. Zhang, H. Huang, C. Dong, X. Dai, G. Feng, L. Lin, D. Sun, D. Yang, L. Xie, Y. Chen, J. Guo and X. Jing, Single Atom-Doped Nanosonosensitizers for Mutually Optimized Sono/Chemo-Nanodynamic Therapy of Triple Negative Breast Cancer, *Adv. Sci.*, 2023, **10**, e2206244.

175 S. Wang, M. Ma, Q. Liang, X. Wu, K. Abbas, J. Zhu, Q. Xu, A. C. Tedesco and H. Bi, Single-Atom Manganese Anchored on Carbon Dots for Promoting Mitochondrial Targeting and Photodynamic Effect in Cancer Treatment, *ACS Appl. Nano Mater.*, 2022, **5**, 6679–6690.

176 Y. Xing, L. Li, Y. Chen, L. Wang, S. Tang, X. Xie, S. Wang, J. Huang, K. Cai and J. Zhang, Flower-like Nanozyme with Highly Porous Carbon Matrix Induces Robust Oxidative Storm against Drug-Resistant Cancer, *ACS Nano*, 2023, **17**(7), 6731–6744.

177 F. Mo, M. Zhang, X. Duan, C. Lin, D. Sun and T. You, Recent Advances in Nanozymes for Bacteria-Infected Wound Therapy, *Int. J. Nanomed.*, 2022, **17**, 5947–5990.

178 M. D. Rojas-Andrade, G. Chata, D. Rouholiman, J. L. Liu, C. Saltikov and S. W. Chen, Antibacterial mechanisms of graphene-based composite nanomaterials, *Nanoscale*, 2017, **9**, 994–1006.

179 C. Jin, S. Fan, Z. Zhuang and Y. Zhou, Single-atom nanozymes: From bench to bedside, *Nano Res.*, 2022, 1–11, DOI: 10.1007/s12274-022-5060-5.


 

180 Y. Zhao, Y. Yu, F. Gao, Z. Wang, W. Chen, C. Chen, J. Yang, Y. Yao, J. Du, C. Zhao and Y. Wu, A highly accessible copper single-atom catalyst for wound antibacterial application, *Nano Res.*, 2021, **14**, 4808–4813.

181 X. Wang, Q. Shi, Z. Zha, D. Zhu, L. Zheng, L. Shi, X. Wei, L. Lian, K. Wu and L. Cheng, Copper single-atom catalysts with photothermal performance and enhanced nanozyme activity for bacteria-infected wound therapy, *Bioact. Mater.*, 2021, **6**, 4389–4401.

182 F. Meng, M. Peng, Y. Chen, X. Cai, F. Huang, L. Yang, X. Liu, T. Li, X. Wen, N. Wang, D. Xiao, H. Jiang, L. Xia, H. Liu and D. Ma, Defect-rich graphene stabilized atomically dispersed Cu3 clusters with enhanced oxidase-like activity for antibacterial applications, *Appl. Catal., B*, 2022, **301**, 120826.

183 X. Feng, J. Lei, L. Ma, Q. Ouyang, Y. Zeng, H. Liang, C. Lei, G. Li, L. Tan, X. Liu and C. Yang, Ultrasonic Interfacial Engineering of MoS(2) -Modified Zn Single-Atom Catalysts for Efficient Osteomyelitis Sonodynamic Ion Therapy, *Small*, 2022, **18**, e2105775.

184 Y. Yu, Y. Cheng, L. Tan, X. Liu, Z. Li, Y. Zheng, T. Wu, Y. Liang, Z. Cui, S. Zhu and S. Wu, Theory-screened MOF-based single-atom catalysts for facile and effective therapy of biofilm-induced periodontitis, *Chem. Eng. J.*, 2022, **431**, 133279.

185 D. Wang, B. Zhang, H. Ding, D. Liu, J. Xiang, X. J. Gao, X. Chen, Z. Li, L. Yang, H. Duan, J. Zheng, Z. Liu, B. Jiang, Y. Liu, N. Xie, H. Zhang, X. Yan, K. Fan and G. Nie, TiO(2) supported single Ag atoms nanozyme for elimination of SARS-$CoV_2$, *Nano Today*, 2021, **40**, 101243.

186 H. Li, M. Sun, H. Gu, J. Huang, G. Wang, R. Tan, R. Wu, X. Zhang, S. Liu, L. Zheng, W. Chen and Z. Chen, Peroxidase-Like FeCoZn Triple-Atom Catalyst-Based Electronic Tongue for Colorimetric Discrimination of Food Preservatives, *Small*, 2023, e2207036, DOI: **10.1002/smll.202207036**.

187 Y. Mao, S. Gao, L. Yao, L. Wang, H. Qu, Y. Wu, Y. Chen and L. Zheng, Single-atom nanozyme enabled fast and highly sensitive colorimetric detection of Cr(VI), *J. Hazard. Mater.*, 2021, **408**, 124898.

188 A. Payal, S. Krishnamoorthy, A. Elumalai, J. A. Moses and C. Anandharamakrishnan, A Review on Recent Developments and Applications of Nanozymes in Food Safety and Quality Analysis, *Food Anal. Methods*, 2021, **14**, 1537–1558.

189 F. Zhang, Y. Li, X. Li, R. Liu, Y. Sang, X. Wang and S. Wang, Nanozyme-enabled sensing strategies for determining the total antioxidant capacity of food samples, *Food Chem.*, 2022, **384**, 132412.

190 E. Ko, W. Hur, S. E. Son, G. H. Seong and D. K. Han, Au nanoparticle-hydrogel nanozyme-based colorimetric detection for on-site monitoring of mercury in river water, *Mikrochim. Acta*, 2021, **188**, 382.

191 Y. Tian, Y. Chen, M. Chen, Z. L. Song, B. Xiong and X. B. Zhang, Peroxidase-like Au@Pt nanozyme as an integrated nanosensor for Ag(+) detection by LSPR spectroscopy, *Talanta*, 2021, **221**, 121627.

192 H. Yang, X. Wu, L. Su, Y. Ma, N. J. D. Graham and W. Yu, The Fe-N-C oxidase-like nanozyme used for catalytic oxidation of NOM in surface water, *Water Res.*, 2020, **171**, 115491.

193 Z. Zhou, M. Li, C. Kuai, Y. Zhang, V. F. Smith, F. Lin, A. Aiello, D. P. Durkin, H. Chen and D. Shuai, Fe-based single-atom catalysis for oxidizing contaminants of emerging concern by activating peroxides, *J. Hazard. Mater.*, 2021, **418**, 126294.

194 Y. Ai, J. You, J. Gao, J. Wang, H.-B. Sun, M. Ding and Q. Liang, Multi-shell nanocomposites based multienzyme mimetics for efficient intracellular antioxidation, *Nano Res.*, 2021, **14**, 2644–2653.

195 L. Sun, W. Li, Z. Liu, Z. Zhou and Y. Feng, Iodine-doped single-atom cobalt catalysts with boosted antioxidant enzyme-like activity for colitis therapy, *Chem. Eng. J.*, 2023, **453**, 139870.

196 Q. Xu, Y. Hua, Y. Zhang, M. Lv, H. Wang, Y. Pi, J. Xie, C. Wang and Y. Yong, A Biofilm Microenvironment-Activated Single-Atom Iron Nanozyme with NIR-Controllable Nanocatalytic Activities for Synergetic Bacteria-Infected Wound Therapy, *Adv. Healthcare Mater.*, 2021, **10**, e2101374.

197 K. Chen, S. Sun, J. Wang and X.-D. Zhang, Catalytic nanozymes for central nervous system disease, *Coord. Chem. Rev.*, 2021, **432**, 213751.

198 X. Gao, W. Ma, J. Mao, C. T. He, W. Ji, Z. Chen, W. Chen, W. Wu, P. Yu and L. Mao, A single-atom Cu-N(2) catalyst eliminates oxygen interference for electrochemical sensing of hydrogen peroxide in a living animal brain, *Chem. Sci.*, 2021, **12**, 15045–15053.

199 Z. Lyu, S. Ding, N. Zhang, Y. Zhou, N. Cheng, M. Wang, M. Xu, Z. Feng, X. Niu, Y. Cheng, C. Zhang, D. Du and Y. Lin, Single-Atom Nanozymes Linked Immunosorbent Assay for Sensitive Detection of Abeta 1–40: A Biomarker of Alzheimer's Disease, *Research*, 2020, **2020**, 4724505.

200 B. Yan, F. Wang, S. He, W. Liu, C. Zhang, C. Chen and Y. Lu, Peroxidase-like activity of Ru-N-C nanozymes in colorimetric assay of acetylcholinesterase activity, *Anal. Chim. Acta*, 2022, **1191**, 339362.

201 G. Song, J. Zhang, H. Huang, X. Wang, X. He, Y. Luo, J. C. Li, K. Huang and N. Cheng, Single-atom Ce-N-C nanozyme bioactive paper with a 3D-printed platform for rapid detection of organophosphorus and carbamate pesticide residues, *Food Chem.*, 2022, **387**, 132896.

202 H. Li, Q. Li, Q. Shi, Y. Wang, X. Liu, H. Tian, X. Wang, D. Yang and Y. Yang, Hemin loaded Zn-N-C single-atom nanozymes for assay of propyl gallate and formaldehyde in food samples, *Food Chem.*, 2022, **389**, 132985.

203 W. Sun, L. Feng, J. Zhang, K. Lin, H. Wang, B. Yan, T. Feng, M. Cao, T. Liu, Y. Yuan and N. Wang, Amidoxime Group-Anchored Single Cobalt Atoms for Anti-Biofouling during Uranium Extraction from Seawater, *Adv. Sci.*, 2022, **9**, e2105008.

204 W. Wei, Single-atom nanozymes towards central nervous system diseases, *Nano Res.*, 2022, 1–19, DOI: **10.1007/s12274-022-5104-x**.

205 P. Muhammad, S. Hanif, J. Li, A. Guller, F. U. Rehman, M. Ismail, D. Zhang, X. Yan, K. Fan and B. Shi, Carbon dots supported single Fe atom nanozyme for drug-resistant glioblastoma therapy by activating autophagy-lysosome pathway, *Nano Today*, 2022, **45**, 101530.
206 S. Zhang, Y. Li, S. Sun, L. Liu, X. Mu, S. Liu, M. Jiao, X. Chen, K. Chen, H. Ma, T. Li, X. Liu, H. Wang, J. Zhang, J. Yang and X. D. Zhang, Single-atom nanozymes catalytically surpassing naturally occurring enzymes as sustained stitching for brain trauma, *Nat. Commun.*, 2022, **13**, 4744.
207 Q. M. Liu and S. W. Chen, Ultrafast synthesis of electrocatalysts, *Trends Chem.*, 2022, **4**, 918–934.
208 T. He, Y. Song, Y. Chen, X. Song, B. Lu, Q. Liu, H. Liu, Y. Zhang, X. Ouyang and S. Chen, Atomically dispersed ruthenium in carbon aerogels as effective catalysts for pH-universal hydrogen evolution reaction, *Chem. Eng. J.*, 2022, **442**, 136337.
209 R. N. Burton-Smith and K. Murata, Cryo-electron microscopy of the giant viruses, *Microscopy*, 2021, **70**, 477–486.
210 J. H. Chen, W. Wang, C. Wang, T. Kuang, J. R. Shen and X. Zhang, Cryo-electron microscopy structure of the intact photosynthetic light-harvesting antenna-reaction center complex from a green sulfur bacterium, *J. Integr. Plant Biol.*, 2023, **65**, 223–234.

 